Middle Triassic (Anisian) Conodont Biostratigraphy at the Shaiwa Section, Guizhou, South China

Binxian Qin[1,2], **Martyn Lee Golding***[3], **Haishui Jiang***[1,2], **Yan Chen**[1,2], **Muhui Zhang**[1,2], **Li Kang**[1,2],
Dacheng Wang[1,2], **Jinling Yuan**[4]

1. *State Key Laboratory of Biogeology and Environmental Geology, China University of Geosciences, Wuhan 430078, China*
2. *School of Earth Sciences, China University of Geosciences, Wuhan 430074, China*
3. *Geological Survey of Canada, Vancouver V6B 5J3, Canada*
4. *Hubei Institute of Geosciences, Wuhan 430034, China*

Binxian Qin: https://orcid.org/0000-0001-8871-9244; Martyn Lee Golding: https://orcid.org/0000-0002-5284-5879;
Haishui Jiang: https://orcid.org/0000-0001-9636-0307

ABSTRACT: The Nanpanjiang Basin is a key area for paleontological and biostratigraphical study of the Middle Triassic. Herein we studied Middle Triassic conodonts from a well-exposed section, the Shaiwa Section, which is located at the northwest end of the Nanpanjiang Basin. A total of six Anisian conodont zones are recognized; in ascending order, they are: the *Nicoraella germanica* Zone, the *Nicoraella kockeli* Zone, the *Paragondolella bulgarica* Zone, the *Neogondolella constricta* Zone, the *Neogondolella cornuta* Zone, and the *Paragondolella excelsa* Zone, respectively. The first occurrence of *Nicoraella kockeli* defines the Bithynian-Pelsonian boundary. The Pelsonian-Illyrian boundary is defined by the first occurrence of *Neogondolella constricta*. The Anisian-Ladinian boundary cannot be recognized at the Shaiwa Section due to the absence of conodont indicative of the Ladinian. However, the new conodont data indicate that the uppermost strata could be very close to the boundary. The abrasion of conodont surfaces provides evidence for demonstrating reworking at the Shaiwa Section, which makes some conodonts possess a longer stratigraphic range than previously recorded. The variation in relative abundance between blade-shaped conodonts and platform conodonts indicates that segminiplanate elements probably preferred deeper and oxygenated environments whereas a restricted marine environment is more suitable for segminate elements.
KEY WORDS: conodont biostratigraphy, Middle Triassic, Shaiwa Section, Nanpanjiang Basin

0 INTRODUCTION

The end-Permian mass extinction is thought to be the most severe biotic crisis of the Phanerozoic, in which over 90% of marine invertebrate taxa were eliminated (e.g., Erwin et al., 2002; Sepkoski, 1984). The alteration of the marine ecosystem structures from Paleozoic-type to Mesozoic-type started here, following several million years of continued catastrophic environmental conditions, until the ecosystem fully recovered in the Middle Triassic (Chen and Benton, 2012). Thus, the Middle Triassic is a key period that recorded the recovery and extensive radiation of the marine biota after the end-Permian mass extinction. Conodonts play important roles in dating and calibrating Middle Triassic strata (Ogg et al., 2016).

The earliest reported conodonts of the Middle Triassic were from the Muschelkalk limestone of Germanic Basin by Tatge (1956), who first described several conodont species, including *Neogondolella mombergensis* and *Nicoraella kockeli*. From then on, Middle Triassic conodonts were identified from the Muschelkalk facies across Europe (e.g., Chen et al., 2019; Escudero-Mozo et al., 2015; Kozur, 2003; Vörös, 2003; Zawidzka, 1975). In North America, Middle Triassic conodonts have been described from the Prida Formation (Fm.) in northwestern Nevada of the USA (Mosher, 1968; Mosher and Clark, 1965), and from the Montney and Doig formations of the western Canada Sedimentary Basin of British Columbia in Canada (Golding, 2018; Golding and Orchard, 2018, 2016; Golding et al., 2014; Orchard and Tozer, 1997). In Asia, Middle Triassic conodonts have been found in Malaysia (Metcalfe, 1990), the Spiti valley of India (Goel, 1977), and the Kiso (Koike et al., 1971), Inuyama and Tsukumi areas (Muto et al., 2019) of Japan. In China, Wang and Wang (1976) first established Middle Triassic conodont zones in the Tulong Group from the Everest (Qomolangma) region, where the *Ng. regale* Zone, the *Ng. constricta* Zone and the *Paragondolella excelsa* Zone were recognized. Subsequently, Middle Triassic conodonts were identified in other regions of Tibet (Xizang) (Wu et al., 2019, 2007; Zhou et al., 2006; Zhao and Zhang, 1991; Tian, 1983), Sichuan (Rao et al., 1985; Wang and Dai, 1981), Guizhou (Liang et al., 2016; Sun et

al., 2014, 2006; Orchard et al., 2007b; Wang et al., 2005; Yao et al., 2004; Wang and Zhong, 1994), Yunnan (e.g., Huang et al., 2009; Zhang et al., 2009; Dong and Wang, 2006; Wang and Zhong, 1994), Guangxi (e.g., Chen et al., 2020; Yan et al., 2015; Wang and Zhong, 1994; Yang et al., 1986), and the Nadanhada Range of Northeast China (Buryi, 1996).

The Nanpanjiang Basin, which was bordered on the north and west by the Yangtze shallow-marine carbonate platform, formed a deep marine embayment in the southern margin of Yangtze Block, and received nearly continuous deposition of deep-marine carbonates and some debris-flow breccia from the adjacent platform throughout Paleozoic to Late Triassic (Fig. 1) (Wang and Shi, 2008; Lehrmann et al., 2003; Wu, 2003). It is an ideal area to study the end-Permian mass extinction and the recovery of marine biotic ecosystems in the Triassic (e.g., Song et al., 2011; Lehrmann et al., 2007; Payne et al., 2006). Numerous Permian and Triassic sections in this basin have been well studied in terms of conodont biostratigraphy (e.g., Liang et al., 2016; Chen et al., 2015; Yan et al., 2015; Wang et al., 2005), magnetostratigraphy (Chen et al., 2020), astrochronology (Li et al., 2018), carbon isotope stratigraphy (e.g., Song et al., 2013; Payne et al., 2004), strontium isotope stratigraphy (Song et al., 2015), geochronology (Ovtcharova et al., 2015; Lehrmann et al., 2006), paleo-seawater temperatures (Sun et al., 2012), and the occurrence of oceanic anoxic events (Song et al., 2012). The Shaiwa Section is located in the northwestern part of the Nanpanjiang Basin, and received continuous deposition from the

Early Permian to the Middle Triassic. Previously, studies at the Shaiwa Section were mainly focused on the Permian (Wang et al., 2016; Ji et al., 2009; Yuan et al., 2009; Gu et al., 2002; Gao et al., 2001; Yang and Gao, 2000) and the Early Triassic strata (Hu et al., 2006). Here we present a detailed Anisian conodont succession at this section for better understanding the Middle Triassic conodonts in South China.

1 GEOLOGICAL SETTING

The Shaiwa Section (25°35′13″N, 106°09′75″E) is located at Shaiwa Village, approximately 3 km northwestern to Sidazhai Town, Ziyun County, about 200 km southwestern of Guiyang City, Guizhou Province (Fig. 1). This section is well exposed and easily accessible, and dominated by marine carbonate sedimentation during the Early–Middle Triassic.

Triassic strata exposed at the Shaiwa Section are represented by the Luolou, Xinyuan and Bianyang formations. The researched Xinyuan Fm. is ~371 m in thickness, which is subdivided into the sandstone member (beds N1–N9, Fig. 2) in the lower part and the limestone member (beds 1–38, Fig. 2) in the upper part (Figs. 3a, 3b). The entire succession records continuous sedimentation in a deeper water environment. The sandstone member is composed of thin- to medium-bedded clastic rock intercalated with thin-bedded or lenticular limestone; fossils are absent in this interval (Figs. 3g, 3h). The thin- to medium-bedded limestone, argillaceous limestone intercalated with thin-bedded mudstone, medium-bedded bioclastic
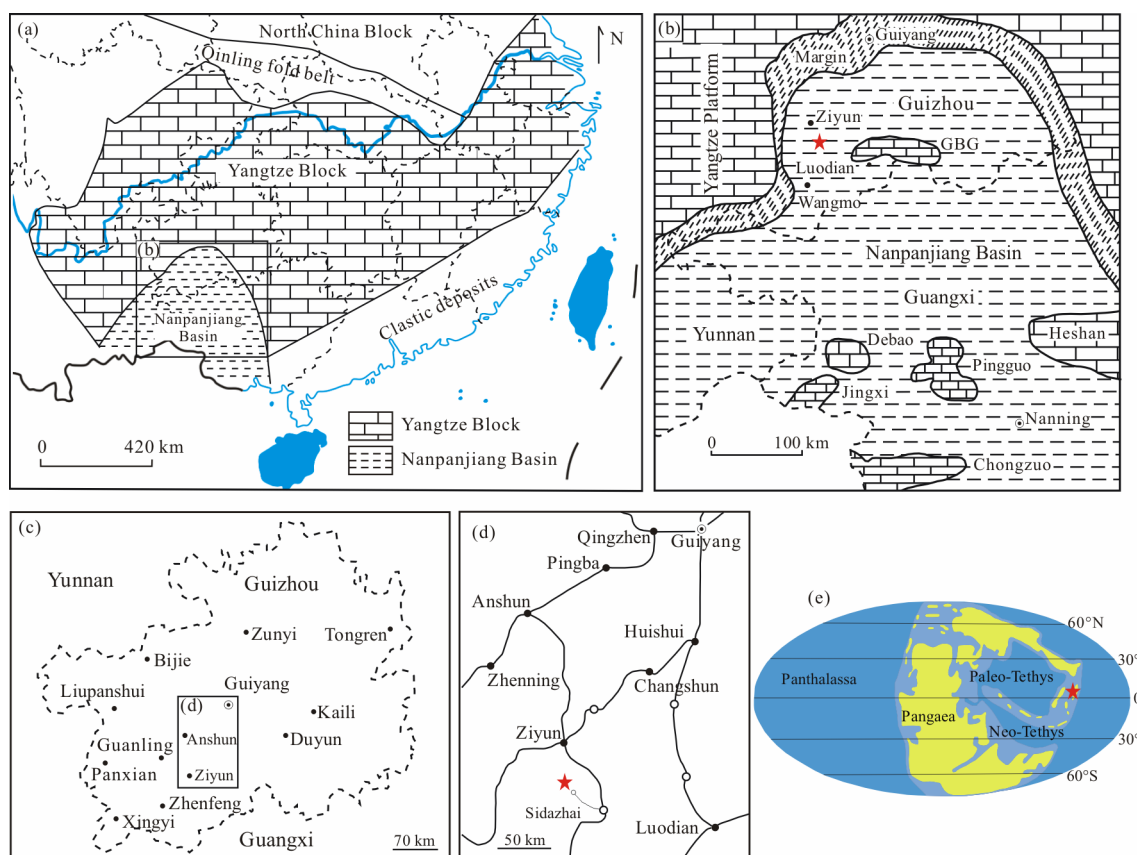

Figure 1. Paleogeography and location of the study section. (a) Paleogeography of the Yangtze Platform and Nanpanjiang Basin; (b) paleogeographical location of the Shaiwa Section (red star) in the Nanpanjiang Basin during the Middle Triassic; GBG. the Great Bank of Guizhou, modified from Lehrmann et al. (2015); (c), (d) location map of the Shaiwa Section; (e) Early–Middle Triassic paleogeography (modified from http://www.scotese.com).
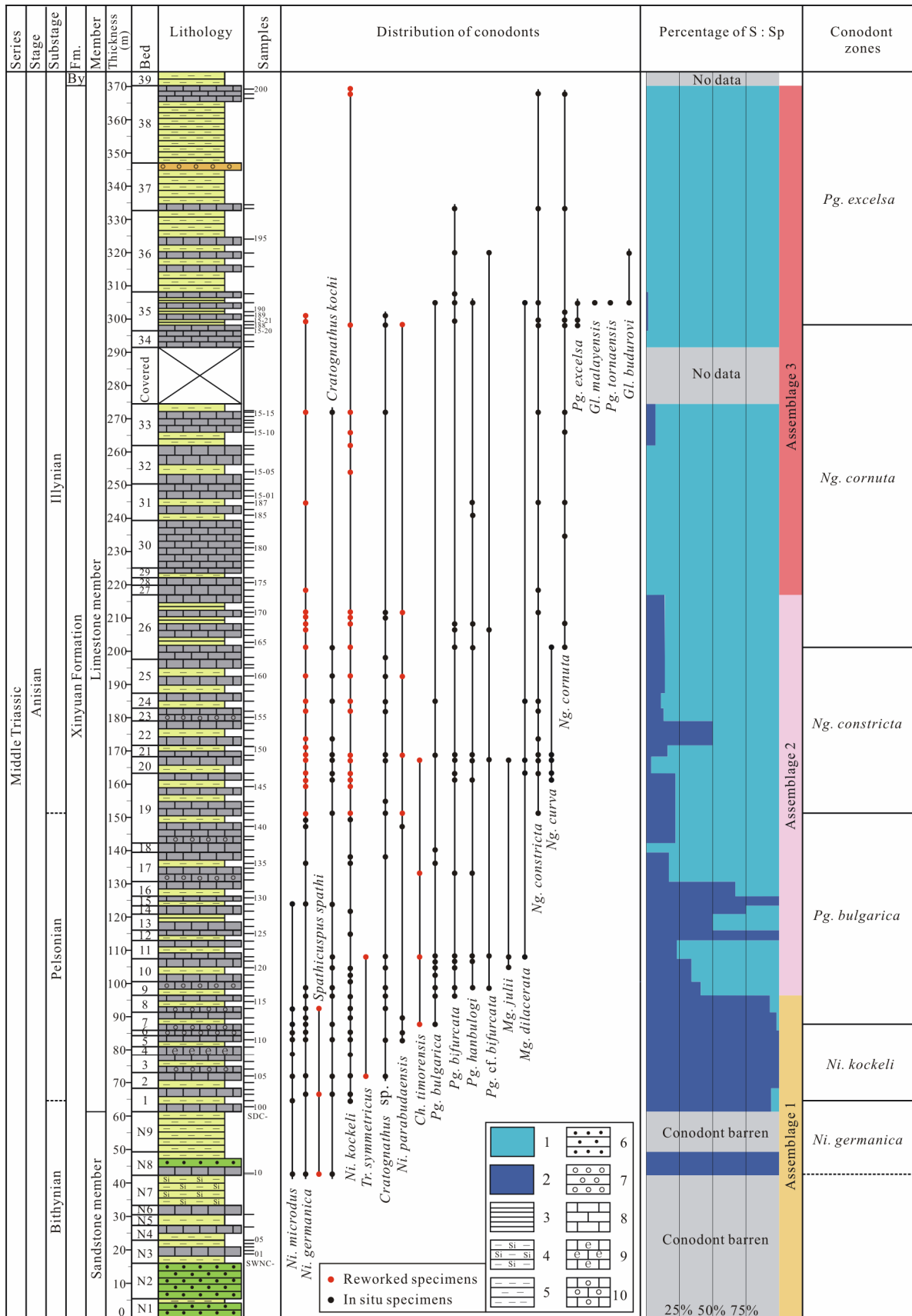
Figure 2. Stratigraphic distribution of Middle Triassic (Anisian) conodonts at the Shaiwa Section. The ratios of segminate and segminiplanate conodonts are shown on the right. 1. Segminiplanate elements (Sp); 2. segminate elements (S); 3. shale; 4. siliceous mudstone; 5. mudstone; 6. sandstone; 7. conglomerate; 8. micrite; 9. bioclastic limestone; 10. calcirudite; *Ch. Chiosella*; *Gl. Gladigondolella*; *Mg. Magnigondolella*; *Ng. Neogondolella*; *Ni. Nicoraella*; *Pg. Paragondolella*; *Tr. Triassospathodus*; Fm. Formation; By. Bianyang Formation.

limestone and calcirudite are predominant in the lower part of the limestone member, whereas the upper part is dominated by thin-bedded mudstone intercalated with limestone, yielding foraminifers, brachiopods, gastropods, ammonoids, ostracods, bivalves and echinoderms (Figs. 3c–3f).

2 MATERIALS AND METHODS

The section was sampled over four field campaigns from 2013 to 2015. A total of 131 rock samples, each weighing about 5 kg, were collected during the field work from the Xinyuan Fm. for conodont extraction. Each sample was crushed into 1.5–2 cm^3 size fragments and dissolved in 10% diluted acetic acid, wet sieved through 20# and 160# meshes and air-dried at room temperature. Subsequently, heavy liquid separation (solution of lithium heteropolytungstates in water) was used to concentrate conodonts from the insoluble residues, following the methods documented by Yuan et al. (2015). Conodonts were then handpicked under a binocular microscope.

3 CONODONT BIOSTRATIGRAPHY

A total of 3 940 conodont specimens were obtained from 70 samples, including about 2 792 P_1 elements (Table 1), among which specimens belonging to the genera can be identified: *Chiosella*, *Cratognathus*, *Gladigondolella*, *Neogondolella*, *Neospathodus*, *Nicoraella*, *Magnigondolella*, *Paragondolella*, *Spathicuspus* and *Triassospathodus*. Based on the stratigraphical distributions of key conodont species, six conodont zones can be established (Fig. 2), as described below. The well-preserved conodont materials (Pl. 1–9) enable us to evaluate the Middle Triassic biostratigraphy at the Shaiwa Section. All specimens are housed at School of Earth Sciences, China University of Geosciences, Wuhan.

3.1 *Nicoraella germanica* Zone

The base of *Ni. germanica* Zone is defined by the first occurrence (FO) of *Ni. germanica*, and the top is defined by the FO of *Ni. kockeli*. At the Shaiwa Section, the FO of *Ni. germanica* is at the base of Bed N8. Since the strata below Bed N8 are mainly composed of clastic rock intercalated with thin-bedded or lenticular limestone, although seven samples were collected in this interval, no conodonts have been retrieved. So, the actual base of this zone at the Shaiwa Section is uncertain while the upper limit is at the base of Bed 1. Associated taxa include *Spathicuspus spathi*, *Ch.* n. sp. A (*sensu* Orchard et al., 2007b), *Ni. microdus*, and *Cratognathus kochi*. Mosher (1968) considered that "*Neospathodus microdus*" was only known from the upper Ladinian. However, Chen et al. (2016) reviewed the evolution of the Middle and early Late Triassic conodonts, suggested that the species "*Nicoraella microdus*" had a stratigraphic range from Bithynian to Pelsonian of Anisian. Other microfossils include fish materials and foraminifers.

The zonal species was originally described by Kozur (1972) from the Lower Muschelkalk of the Germanic Basin and was used to define the *Ni. germanica* Zone, which characterized the Bithynian Substage in the Germanic Basin. Outside the Germanic Basin, this species was only found in a few areas of Tethys and western Panthalassa (Nicora, 1977). In China, *Ni. germanica* was identified from the Leikoupo Fm. in Sichuan

(Wang and Dai, 1981), the Guanling Fm. in Guizhou (Sun et al., 2009) and Yunnan (Huang et al., 2011; Zhang et al., 2009), the Luolou Fm. (Wang et al., 2005) and the Poduan Fm. (Liang et al., 2016) in Guizhou, the Gejiu Fm. and Huoma Fm. (Dong and Wang, 2006; Wang and Zhong, 1994) in Yunnan, and the Baifeng Fm. in Guangxi (Yang et al., 1986).

Table 1 Numerical distribution of segminiplanate elements (Sp) and segminate elements (S) at the Shaiwa Section. The numbers in parentheses are *in situ* specimens

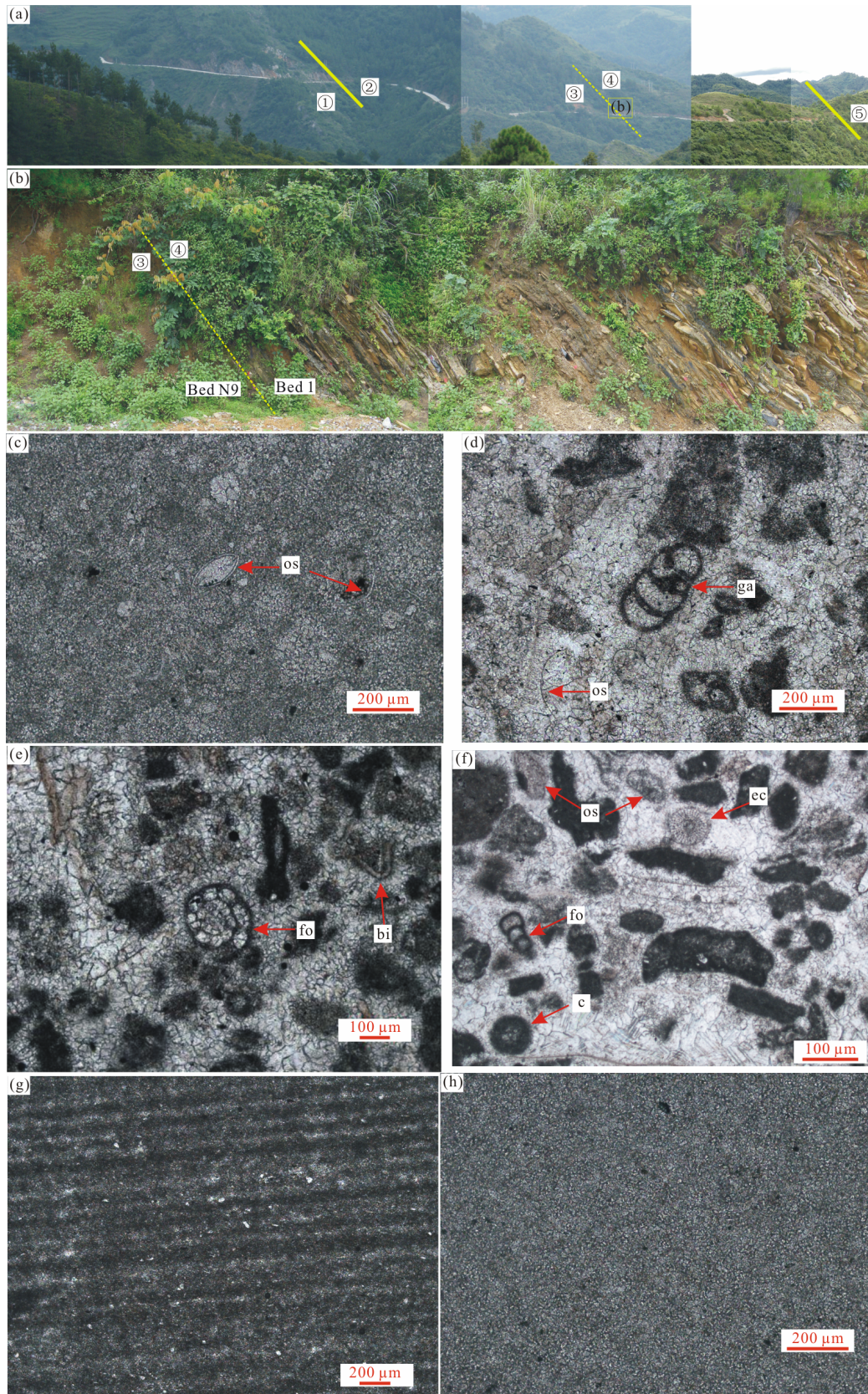| Bed	Sp	S	Ramiform	Total	Sp : S	S : Sp
38	4(4)	11(0)	31	46	100	0
37	4(4)	0(0)	16	20	100	0
36	9(9)	0(0)	3	12	100	0
35	138(136)	37(2)	58	233	98.551	1.449
34	3(3)	1(0)	0	4	100	0
33	53(53)	32(4)	73	158	92.982	7.018
32	1(1)	4(0)	10	15	100	0
31	50(50)	10(0)	22	82	100	0
30	2(2)	0(0)	1	3	100	0
29	0(0)	0(0)	0	0	100	0
28	1(1)	2(0)	0	3	100	0
27	2(2)	6(0)	9	17	100	0
26	121(119)	738(20)	108	967	85.612	14.388
25	12(12)	41(2)	37	90	85.714	14.286
24	67(65)	71(8)	40	178	89.041	10.959
23	27(27)	30(4)	41	98	87.097	12.903
22	2(2)	5(2)	2	9	50	50
21	56(55)	73(11)	66	195	83.333	16.667
20	51(46)	28(2)	69	148	95.833	4.167
19	90(88)	288(26)	237	615	77.193	22.807
18	2(2)	0(0)	2	4	100	0
17	134(133)	27(26)	40	201	83.75	16.250
16	1(1)	2(2)	0	3	33.333	66.667
15	0(0)	22(22)	14	36	0	100
14	1(1)	3(3)	0	4	25	75
13	1(1)	1(1)	1	3	50	50
12	0(0)	2(2)	40	42	0	100
11	40(39)	33(12)	2	75	76.471	23.529
10	28(28)	17(15)	59	104	65.116	34.884
9	17(17)	14(12)	3	34	58.621	41.379
8	2(2)	31(30)	46	79	6.25	93.750
7	1(1)	54(48)	37	92	2.041	97.959
6	0(0)	53(51)	7	60	0	100
5	0(0)	123(117)	3	126	0	100
4	0(0)	7(5)	0	7	0	100
3	0(0)	2(2)	0	2	0	100
2	0(0)	36(32)	4	40	0	100
1	1(1)	19(16)	31	51	5.882	94.118
N6	0(0)	48(38)	36	84	0	100
Total	921(905)	1	1 148	3	\	\

Figure 3. Outcrop and thin section photographs of the Xinyuan Formation. (a) The panorama of the Shaiwa Section; (b) outcrop view boundary of the sandstone member and the limestone member; (c)–(f) thin sections of bioclastic limestone from the limestone member; (g)–(h) thin sections of micrite limestone from the sandstone member, both thin sections consist of fine micrite calcite and lack bioclastic. ① Luolou Formation; ② Xinyuan Formation; ③ sandstone member; ④ limestone member; ⑤ Bianyang Formation. Abbreviations: bi. bivalve; br. brachiopod; c. Tubiphytes; ec. echinoderm; fo. foraminifer; ga. gastropod; os. ostracod.

Nicoraella germanica is identified as an index fossil of the Bithynian (Narkiewicz and Szulc, 2004; Yang et al., 1999), i.e., the second substage of the Anisian stage, Middle Triassic (Ogg et al., 2014). The first appearance of this species has been interpreted as indicating the base of the Bithynian (Lehrmann et al., 2015, 2006; Kozur, 2003). In North America, *Ni. germanica* has a first rare occurrence in the beds corresponding to the uppermost Aegean ammonoid *Pseudokeyserlingites guexi* Zone and becomes common in the succeeding lowest Bithynian ammonoid *Siberlingites mulleri* Zone (Nicora, 1977). However, the first appearance datum of this species in the Germanic Basin is late Bithynian, rather than early Bithynian (Narkiewicz and Szulc, 2004); this phenomenon is also supported by the conodont succession from Silesia, where *Ni. germanica* first appears in the latest Bithynian (Zawidzka, 1975) and the Holy Cross Mountains, where the first appearance is as late as the Pelsonian (Trammer, 1975). The interpretation of this phenomenon is that those areas were in restricted marine environmental conditions in the late Bithynian, that was more suitable for the late development of *Nicoraella* (Narkiewicz and Szulc, 2004).

3.2 *Nicoraella kockeli* **Zone**

The lower limit of this zone is defined by the FO of *Ni. kockeli* in Bed 1, and the upper limit is marked by the FO of *Paragondolella bulgarica* at the base of Bed 7. Conodonts from this zone include the relatively abundant *Ni. kockeli* and its antecessor *Ni. germanica*, as well as transitional forms between *Ni. germanica* and *Ni. kockeli*. One platform element was found in this zone (Plate 4, 10a–10c). The other associated conodont species include *Ni. microdus*, *Ni. parabudaensis*, *Ch.* n. sp. A, *Cratognathus kochi*, *Triassospathodus symmetricus*, *Tr. homeri*, and *Cratognathus* sp.. Other microfossils in this zone mainly include fish materials and foraminifers.

Huang et al. (2011, 2009) distinguished two morphotypes of *Ni. kockeli* based on the different basal cavity in P$_1$ elements: *Ni. kockeli* type 1 (the basal margin is straight) and *Ni. kockeli* type 2 (the anterior and posterior basal margin is straight while the basal cavity has a curved appearance). These two morphotypes are also identified in our material (Plate 2, type 1: 11, 12, 17–19, 21; type 2: 13–16, 20, 22, 23).

Nicoraella kockeli was thought to have evolved from *Ni. germanica* (Sun et al., 2006; Narkiewicz and Szulc, 2004; Meco, 1999; Trammer, 1975), which was first reported from the lower Muschelkalk of the Germanic Basin in German (Tatge, 1956) and characterizes the Pelsonian both in the Germanic Basin and the Tethyan oceanic areas (Kozur, 2003; Nicora, 1977). Subsequently, this species has been widely identified in Nevada of the USA (Carey, 1984; Nicora, 1977), Malaysia (Metcalfe, 1990), Poland (Narkiewicz and Szulc, 2004; Narkiewicz, 1999; Trammer, 1975, 1972, 1971; Zawidzka, 1975), Austria (Kozur et al., 1994), Albania (Meco, 1999), and the Balaton Highland in Hungry (Vörös, 2003). In China, the *Ni. kockeli* Zone is present in the Guanling Fm. in Guizhou (Sun et al., 2014, 2006; Wang and Zhong, 1994) and Yunnan (Huang et al., 2009), the Luolou Fm. and the Guandao wedges (Wang et al., 2005), the Poduan Fm. (Liang et al., 2016) in Guizhou, the Baifeng Fm. (Yang et al., 1986) in Guangxi, and the Huoma Fm. (Dong and Wang, 2006) in Yunnan. The strati-

graphic range of this species encompasses the entire Pelsonian (Narkiewicz, 1999).

3.3 *Paragondolella bulgarica* **Zone**

The *Pg. bulgarica* Zone begins with the FO of *Pg. bulgarica* and ends with the FO of *Ng. constricta*, ranging from Bed 7 to the lower part of Bed 19. The conodonts are abundant and diverse in this zone. Associated taxa include *Ni. kockeli*, *Ni. germanica*, *Ni. microdus*, *Ni. parabudaensis*, *Ns. excelsus*, *Tr. symmetricus*, *Ch. timorensis*, *Spathicuspus spathi*, *Cratognathus kochi*, *Pg. bifurcata*, *Pg. hanbulogi*, *Magnigondolella* (*Mg.*) *dilacerata*, *Mg. julii*, and *Cratognathus* sp.. Other microfossils are mainly fish materials.

Paragondolella bulgarica is a widespread species in Middle Triassic strata, which was originally reported from the Golo-Bardo Mountains in Bulgaria (Budurov and Stefanov, 1972). This species is also found in the Holy Cross Mountains and the Muschelkalk facies in Poland (Narkiewicz and Szulc, 2004; Trammer, 1975, 1972; Zawidzka, 1975) and eastern Iberia (Escudero-Mozo et al., 2015), the pelagic strata of Albania (Meco, 1999), Nevada of the USA (Nicora, 1977), northeastern Spain (Márquez-Aliaga et al., 2000), and the Balaton Highland in Hungry (Vörös, 2003). In China, *Pg. bulgarica* was recorded in the Guanling Fm. (Sun et al., 2014, 2006), the Xinyuan Fm. (Xie et al., 2019; Ding and Huang, 1990), the Poduan Fm. (Bo et al., 2017), the Qingyan Fm. (Ji et al., 2011), the Yangliujing Fm. (Chen and Wang, 2009) and the Guandao wedges (Wang et al., 2005) in Guizhou. The stratigraphic range of this species is from Bithynian to lower Illyrian (Márquez-Aliaga et al., 2000; Trammer, 1972).

In the Germanic Basin, the appearance of *Pg. bulgarica* is contemporaneous with that of *Ni. germanica* within the Bithynian (Narkiewicz and Szulc, 2004), and the *Pg. bulgarica* Zone is contemporaneous with the *Ni. germanica* Zone and the succeeding *Ni. germanica-Ni. kockeli* assemblage zone (Kozur, 2003). In China, the *Ni. germanica* Zone and the *Ni. kockeli* Zone are generally representative of platform facies, whereas the *Pg. bulgarica* Zone indicates basin facies (Yang et al., 1999). At the Shaiwa Section, in ascending order, the *Ni. germanica* Zone, the *Ni. kockeli* Zone and the *Pg. bulgarica* Zone can be identified, respectively. A similar conodont succession was recognized at the Guandao Section (Lehrmann et al., 2015; Wang et al., 2005). Therefore, the conodont succession at the Shaiwa Section can be well correlated with that at the Guandao Section (Fig. 4).

The genus *Magnigondolella* was established by Golding and Orchard (2018) from the Anisian of British Columbia in Canada and Nevada in the USA. This genus is characterized by species with high and fused carinas, which were previously referred to *Neogondolella* ex gr. *regalis* (e.g., Lehrmann et al., 2015). This uniformly high, fused carina distinguishes *Magnigondolella* from *Neogondolella*. The genus *Paragondolella* is similar to *Magnigondolella* in the height and fusion of its carina; nevertheless, the highest part of the carina is at the mid point and it descends to both sides of the element in contrast to that of *Magnigondolella*. *Magnigondolella dilacerata* was originally assigned to *Ng. dilacerata* (Golding and Orchard, 2016) and was later placed into *Magnigondolella* by Golding and Orchard (2018) due to its uniformly high and fused carina. This species is characterized by an asymmetrical posterior

Age	Shaiwa (Guizhou) This study	Guandao (Guizhou) Wang et al. (2005)	Guandao Lehrmann et al. (2015)	Yangjuan-Chupiwa (Guizhou) Sun et al. (2014)	Pojiao (Guizhou) Xie et al. (2019)	Yunnan Dong and Wang (2006)	British Columbia, Canada Orchard and Tozer (1997)	British Columbia, Canada Golding et al. (2014) Conodont faunal assemblage	Integrated zones Kozur (2003)
Anisian — Illyrian	*Pg. excelsa*		*Pg. excelsa*			*Pg. ex gr. excelsa*	*Ng. aldae*	*Pg. ex gr. liebermani*	*Ng. mesotriassica*
Anisian — Illyrian	*Ng. cornuta*	*Ng. constricta cornuta*	*Ng. constricta*	*Ng. constricta cornuta*	*Ng. constricta cornuta*		*Ng. constricta*	*Pg. ex gr. liebermani*	*Ng. constricta*
Anisian — Illyrian	*Ng. constricta*	*Ng. constricta*	*Ng. constricta*	*Ng. constricta*	*Ng. constricta*	*Ng. constricta*	*Ng. constricta*		*Ng. constricta*
Anisian — Pelsonian	*Pg. bulgarica*	*Pg. bulgarica*	*Pg. bulgarica*	*Pg. bifurcata*	*Pg. bifurcata*	*Pg. bifurcata*	*Ng. shoshonensis*	*Ng. ex gr. shoshonensis*	*Pg. bifurcata*
Anisian — Pelsonian					*Pg. bulgarica*	*Pg. bulgarica*			*Ni. germanica-Ni. kockeli*
Anisian — Pelsonian	*Ni. kockeli*	*Ni. kockeli*	*Ni. kockeli*	*Ni. kockeli*	*Ni. kockeli*	*Ng. ex gr. regalis*	*Ng. ex gr. regalis* / *Ng. n. sp. N*	*Ng. ex gr. regalis* C / *Ng. n. sp. N* / *Ng. ex gr. regalis* B	*Ni. germanica-Ni. kockeli*
Anisian — Bithynian	*Ni. germanica*	*Ni. germanica*	*Ni. germanica*	*Ni. germanica*	*Ni. germanica*		*Ng. n. sp. M*	*Ng. ex gr. regalis* D / *Ng. sp. n. M*	*Ni. germanica*

Figure 4. Correlation of the Middle Triassic (Anisian) conodont zonations. Abbreviations: *Ng. Neogondolella*; *Ni. Nicoraella*; *Pg. Paragondolella*.

platform, an equal size of cusp and posterior denticle, strong fusion of the posterior two thirds of the carina, and has a stratigraphic range from the ammonoid *Lenotropites caurus* Zone (*Grambergia nahwisi* Subzone) to *Paracrochordiceras americanum* Zone of the lower Anisian in North America (Golding and Orchard, 2016). *Magnigondolella julii* ranges from the ammonoid *Lenotropites caurus* Zone to the upper Anisian (Golding and Orchard, 2018). In our materials, some specimens of *Mg. julii* are similar to *Ng. constricta* but can be distinguished from the latter by the high and fused carina (Plate 4, 8a–8c).

3.4 *Neogondolella constricta* Zone

The *Ng. constricta* Zone begins with the FO of *Ng. constricta* in Bed 19 and ends with the FO of *Ng. cornuta* in the lower part of Bed 26. The associated taxa include *Ni. kockeli*, *Ni. germanica*, *Ni. parabudaensis*, *Cratognathus kochi*, *Ch. timorensis*, *Mg. dilacerata*, *Pg. bulgarica*, *Pg. bifurcata*, *Pg. hanbulogi*, *Mg. julii*, *Ng. curva*, and *Cratognathus* sp. Other microfossils are mainly fish materials and foraminifers.

Since *Ng. constricta* was first identified by Mosher and Clark (1965) in northwestern Nevada of the USA, this species has been widely recognized over the world, for instance in Poland (Narkiewicz, 1999; Trammer, 1975), Austria (Kozur et al., 1994; Mosher, 1968), northeastern Spain (Márquez-Aliaga et al., 2000), the Balaton Highland in Hungry (Kovács, 1994; Kovács et al., 1990), southern Alps (Kovács et al., 1990), eastern Iberia in the western Tethys (Escudero-Mozo et al., 2015), and the western Canada Sedimentary Basin (Orchard and Tozer, 1997). In China, the *Ng. constricta* Zone has been reported from the Xinyuan Fm. (Xie et al., 2019; Ding and Huang, 1990), the Qingyan Fm. (Qin et al., 1993), the Xuman Fm. (Wang, 1996), the Guandao wedges (Wang et al., 2005), the Longtou Fm. (Wu et al., 2008), the Guanling Fm. (Sun et al., 2014, 2006) and the Poduan Fm. (Bo et al., 2017) in Guizhou, the Banna Fm. and Lanmu Fm. (Wang and Zhong, 1994) in Guangxi, the Falang Fm. and Gejiu Fm. (Dong and Wang, 2006; Wang and Zhong, 1994) in Yunnan, and the Tulong Group from the Everest (Qomolangma) region of Tibet (Xizang) (Zhou et al., 2006; Wang and Wang, 1976).

Neogondolella constricta is a comprehensive species that is typical of the Illyrian (Orchard, 2010). In North America and Tethys, the stratigraphic range of this species spans the middle-upper parts of the Illyrian to the Fassanian (Ladinian stage)

(Lehrmann et al., 2015; Márquez-Aliaga et al., 2000; Yang et al., 1999; Mosher, 1968), corresponding to the upper parts of *Paraceratites trinodosus* to *Eoprotrachyceras curioni* ammonoid zones (Márquez-Aliaga et al., 2000). However, some scholars have demonstrated that this taxa appeared well below the Anisian-Ladinian boundary (Orchard, 2010; Kozur, 2003; Wang and Wang, 1976), suggesting even perhaps that the upper range-limit of this taxa does not overstep the Illyrian ammonoid *Paraceratites* beds (Kozur et al., 1994), whereas the lower limit may extend to the latest Pelsonian (Lehrmann et al., 2015; Sun et al., 2006).

The associated species *Ng. curva* was first introduced by Golding and Orchard (2016) from British Columbia of Canada and Nevada of the USA, where the stratigraphic range corresponds to the ammonoid *Lenotropites caurus* Zone to *Hollandites minor* Zone and *Pesudodanubites nicholsi* Subzone to *Augustaceras escheri* Subzone respectively.

3.5 *Neogondolella cornuta* **Zone**

The *Ng. cornuta* Zone ranges from the lower part of the Bed 26 to the lower part of Bed 35. The lower limit of this zone is defined by the FO of *Ng. cornuta* and the top is marked by the FO of *Pg. excelsa*. Co-occurring conodonts are *Ni. kockeli*, *Ni. germanica*, *Ni. microdus*, *Ni. parabudaensis*, *Cratognathus kochi*, *Ng. constricta*, *Ng. curva*, *Ng. longa*, *Pg. bifurcata*, *Pg. hanbulogi*, and *Cratognathus* sp..

Neogondolella cornuta was originally identified from the Golo-Bardo Mountains in Bulgaria (Budurov and Stefanov, 1972) and is very common in the Illyrian ammonoid *Paracetatites-Reitziites* bed (Brack et al., 2005; Kovács, 1994; Kozur et al., 1994). The last appearance datum of this species is considered to be below the Anisian-Ladinian boundary (Chen et al., 2016; Brack et al., 2005) and the *Ng. cornuta* Zone represents the upper part of the Illyrian (Budurov and Stefanov, 1972). In China, the *Ng. cornuta* Zone was previously regarded as the *Ng. constricta cornuta* Zone, which could be recognized from the Guandao wedges (Wang et al., 2005), the Xinyuan Fm. (Xie et al., 2019) and the lower part of Yangliujing Fm. (Sun et al., 2014) in Guizhou, corresponding to the upper part of the Anisian.

It is noteworthy that Kovács (1994) suggested that *Ng. cornuta* and *Ng. balkanica* (Budurov and Stefanov, 1975) were morphotypes of *Ng. constricta*. However, Kozur et al. (1994) differentiated these three species based on the outline of platform of which *Ng. constricta* possesses a distinct constricted posterior platform, *Ng. balkanica* has a slender platform and an erect cusp surrounded by a distinct platform brim, whereas *Ng. cornuta* displays a posteriorly inclined cusp fused with the platform end. In our materials, *Ng. constricta* and *Ng. cornuta* are recognized whereas *Ng. balkanica* cannot be identified in terms of the description by Kozur et al. (1994).

3.6 *Paragondolella excelsa* **Zone**

The FO of *Pg. excelsa* defines the base of this zone in the lower part of Bed 35 and its upper limit is not defined because the beds above this horizon are devoid of index conodonts. The abundance and diversity of blade-shaped conodonts decrease in this zone, as only *Ni. kockeli* and *Cratognathus* sp. are recognized. Other associated conodont species include *Gladigondolella malayensis*, *Gl. budurovi*, *Ng. constricta*, *Ng. cornuta*,

Mg. dilacerata, *Ng. longa*, *Pg. bifurcata*, *Pg. bulgarica*, *Pg. hanbulogi*, and *Pg. tornaensis*. Other microfossils are mainly fish materials and ostracodes.

Mosher (1968) first introduced the zonal species in Europe and Western North America, which first appeared in the upper Anisian. Later, the *Pg. excelsa* Zone was also identified in other areas of the Europe (Zawidzka, 1975; Budurov and Stefanov, 1972) and the pelagic deep-sea bedded chert of Kiso and Tsukumi areas in Japan (Muto et al., 2019; Koike et al., 1971). In China, *Pg. excelsa* was recognized from the Tulong Group in Tibet (Xizang) (Tian, 1983; Wang and Wang, 1976), the Xinyuan Fm. (Wang, 1996), the Guanling Fm. (Sun et al., 2014), the Bianyang Fm. (Qin et al., 1993), the lower-middle part of Lanmu Fm. (Wang and Zhong, 1994) and the Xuman Fm. (Wang, 1996) in Guizhou, and the uppermost part of the Banna Fm. in Guangxi (Wang and Zhong, 1994).

In China, the *Pg. excelsa* Zone was used instead of the *Ng. mombergensis* Zone as the first conodont zone of the Ladinian (Wang, 1991) whereas in Guandao Section, the *Pg. excelsa* Zone was regarded as the latest zone of Anisian (Lehrmann et al., 2015). The stratigraphic range of *Pg. excelsa* is considered to span the upper Illyrian to lower Fassanian (Orchard, 2010; Kozur et al., 1994). In China, this species appears to range from the Anisian ammonoid *Ptychites rugifer* Zone to the Ladinian *Paraceratites ladinum* Zone (Wang and Wang, 1976).

The P_1 element of *Gladigondolella* is characterized by discrete, low and rounded carina nodes. This genus is considered to be a pelagic conodont which is restricted to the Tethys, a few areas of Panthalassa and the western margin of North America. The species *Gl. malayensis* (Nogami, 1968) is thought to be restricted to the Tethys (Orchard, 2010), with a stratigraphic range from late Ladinian to Carnian (e.g., Chen et al., 2016; Balini et al., 2000; Nogami, 1968). However, the oldest records of this species appear in the upper Anisian, equivalently to the *Reiziites reitzi* Zone (see Orchard, 2010, fig. 8). Many studies have documented *Gl. malayensis* in parts of Tethys and Panthalassa (e.g., Zhang et al., 2019; Hornung, 2006) whereas it is very rarely reported from South China. Zhang et al. (2017) documented *Gl. malayensis* from the Zhuganpo Fm. in Guizhou Province and assigned it to the Julian substage, Carnian. Balini et al. (2000) and Chen et al. (2016) noted that the species *Gl. budurovi* (Kovács and Kozur, 1980) is morphologically very similar to *Gl. malayensis*; however, it can be distinguished from the latter by its shorter, thicker and broader platform, lower carina, an undeveloped cusp and a subterminal basal cavity, and a stratigraphic range that is restricted to the Anisian (Zhang et al., 2017; Chen et al., 2016). In our materials, both of these species are able to be identified, of which *Gl. malayensis* (Plate 4, 6a–6c) possessed a more slender, longer platform and a more developed cusp, distinguishing it from *Gl. budurovi* (Plate 4, 1–5).

4 DISCUSSION
4.1 Stage/Substage Boundaries
4.1.1 The Bithynian-Pelsonian boundary

Previously, the base of Pelsonian has been identified by the first occurrence of ammonoid *Balatonites balatonicus* in the area of the Balaton Highlands in Hungary (Vörös, 2003). Lehrmann et al. (2015) constrained the Bithynian-Pelsonian

boundary at an uncertain horizon between the last occurrence of *Ng.* ex gr. *regalis* and the first occurrence of *Pg. bulgarica*, and suggested using the first occurrence of *B. balatonicus* accompanied by *Pg. bulgarica* as the proxy for the base of the Pelsonian. At the Shaiwa Section, however, the appearance of *Pg. bulgarica* is lower than the appearance of *Ng.* ex gr. *regalis* (assigned to the genus *Magnigondolella* in this study), and it appears as though *Pg. bulgarica* occurs higher than other Pelsonian species such as *Ni. kockeli* (Fig. 2). Therefore, the first occurrence of *Pg. bulgarica* does not indicate the Bithynian-Pelsonian boundary at the Shaiwa Section.

The usage of the first occurrence of *Ni. kockeli* as the proxy for the base of the Pelsonian has been supported by numerous publications due to its wide distribution (e.g., Liang et al., 2016; Lehrmann et al., 2006; Narkiewicz, 1999). In Southwest China, the Panxian Fauna in Guizhou (Hao et al., 2006; Sun et al., 2006) and the Luoping Biota in Yunnan (Huang et al., 2011, 2009; Zhang et al., 2009) are restricted to the *Ni. kockeli* Zone and are interpreted to be Pelsonian. At the Shaiwa Section, the first occurrence of *Ni. kockeli* is at the base of Bed 1; above this horizon, the lithology is dominated by limestone, which is significantly different from the underlying strata dominated by clastic rock (Fig. 2), indicating transgressive conditions that enabled a rapid dispersal of *Ni. kockeli* in the Pelsonian (Narkiewicz and Szulc, 2004). Consequently, the first occurrence of *Ni. kockeli* at the base of Bed 1 is interpreted as marking the Bithynian-Pelsonian boundary at the Shaiwa Section.

4.1.2   The Pelsonian-Illyrian boundary

The Pelsonian-Illyrian (middle/upper Anisian) boundary is typically placed at the horizon between the ammonoids *Bulogites zoldianus* Zone and *Rieppelites cimeganus* Zone, which is characterized by the disappearance of *Acrochordiceras*, *Balatonites* and *Bulogites* and the appearance of *Rieppelites* (Monnet et al., 2008). Lehrmann et al. (2015) placed the Pelsonian-Illyrian boundary at the first occurrence *Pg. excelsa* at the Guandao Section, slightly higher than the first occurrence of *Ng. constricta*, suggesting this horizon approximates the transition from the *Bulogites zoldianus* Zone to the *Rieppelites cimeganus* Zone. At the Shaiwa Section, the first occurrence of *Ng. constricta* is also lower than the first occurrence of *Pg. excelsa*, and the typical Illyrian *Ng. cornuta* Zone is recognized between the *Ng. constricta* Zone and the *Pg. excelsa* Zone. Thus, at the Shaiwa Section, the Pelsonian-Illyrian boundary is placed at the lower part of Bed 19, on the basis of the first occurrence of *Ng. constricta*.

4.1.3   The Anisian-Ladinian boundary

The Anisian-Ladinian (A-L) boundary is defined based on the first appearance of the ammonoid *Eoprotrachyceras curionii* or the lowest occurrence of the conodont *Budurovignathus praehungaricus* near the top of ammonoid *Nevadites secedensis* Zone in the uppermost Anisian (Orchard, 2010; Brack et al., 2005). Unfortunately, neither of the above ammonoid or conodont has yet been discovered in China. The first occurrence of the conodont *Bv. truempyi*, the successor species of *Bv. praehungaricus*, is within the *E. curionii* Zone (Muttoni et al., 2004). This species was used as the proxy for the A-L boundary at the Guandao Sec-

tion (Lehrmann et al., 2015; Wang et al., 2005). At the Shaiwa Section, *Bv. truempyi* has not been retrieved.

Brack et al. (2005) and Chen et al. (2016) suggested that *Ng. cornuta* does not occur above the A-L boundary. At the Shaiwa Section, the latest appearance of *Ng. cornuta* is at the top-most of the Xinyuan Fm. (Fig. 2). Consequently, the A-L boundary cannot be recognized at the Shaiwa Section. Tong et al. (2019) suggested that the FAD of *Pg. excelsa* can be a useful proxy for the base of the "Xinpuan" age (a Chinese stage equivalent to the Ladinian stage) in China. In addition, the *Pg. excelsa* Zone was adopted as the first conodont zone of the Ladinian (Wang, 1991). However, although *Pg. excelsa* is often more abundant near the A-L boundary, it appears well below the boundary and ranges across it (Orchard, 2010; Lai and Mei, 2000). At the Shaiwa Section, the first occurrence of *Pg. excelsa* is at the lower part of Bed 35. Therefore, the uppermost stratum of Shaiwa Section may be very close to the boundary between the Anisian and the Ladinian.

4.2   On the Problem of Stratigraphic Ranges of Some Conodonts

The genus *Triassospathodus* is characterized by an inconspicuous cusp and a straight or slightly downward curved posterior end of the lower margin (Kozur et al., 1998), and ranges from the upper Olenekian (Spathian) to the lowermost Anisian (Aegean) (Chen et al., 2016; Goudemand et al., 2012; Orchard et al., 2007a, b; Wang et al., 2005). In our research, this genus has a longer range than previous reports, and the youngest record is Pelsonian (Fig. 2). The genus *Chiosella* is characterized by its mid-lateral rib and lack of platform on the P_1 element, with a stratigraphic range from the uppermost Spathian to Aegean (Chen et al., 2016). However, Wang et al. (2005) documented that *Ch. timorensis* co-occurred with *Ni. kockeli* in Guandao wedges, and the youngest record of this species appeared in the Pelsonian (Liang et al., 2016; Orchard et al., 2007b). At the Shaiwa Section, the latest occurrence of *Ch. timorensis* is in the *Ng. constricta* Zone, which is equivalent to the lower part of the Illyrian (Fig. 2, Plate 3, 2a–2d). The P_1 element of *Spathicuspus spathi* (Sweet, 1970) is a small segminate element with a large prominent cusp and a few posterior denticles, which ranges from the Spathian to the basal Anisian, where is overlaps with the appearance of *Gl. tethydis* (Huckriede, 1958) (Orchard, 2010; Orchard et al., 2007b; Wang et al., 2005). The population of this species increases first followed by a rapid disappearance within the Olenekian-Anisian boundary interval (Orchard et al., 2007b). However, at the Shaiwa Section, the latest record of this species is in Bed 8 (Fig. 2), corresponding to the lower part of Pelsonian. The genus *Nicoraella* was originally assumed to have evolved from the genus *Neospathodus* (Kozur, 1989), and is considered to be one of the most significant conodont genera for the Middle Triassic, and its stratigraphic range does not extend beyond the Pelsonian (Chen et al., 2016). The Early Carnian species *Nicoraella postkockeli* (Kozur, 1993) was assigned to the genus *Mosherella* (Orchard, 2005) based on its evolutionary lineage (Chen et al., 2016). In our materials, the range of *Nicoraella* spans the whole section, and the youngest representative of this genus is Illyrian (Fig. 2 and Plate 2, 24).

As noted above, the stratigraphic ranges of these recorded conodonts are inconsistent with previous studies. Indeed, the longer stratigraphic range or mixing of various conodonts identified at the Shaiwa Section is likely explained by the reworking of some specimens. As is well known, conodonts are composed of apatite, which is highly resistant to destruction by weathering and the preservation of conodonts can indicate the sedimentary setting. The processing of conodonts from host rock could damage the specimens (i.e., loss or breakage of platform or denticles), nevertheless, by contrast, the abrasion of the conodont surface is likely to indicate that the fossils were transported before being deposited. In our materials, these abrasions are found both in segminiplanate and segminate elements, spanning from the base to the top of the section (Figs. 2 and 5). In addition, the presence of conglomerate in the current section provides another evidence for reworking. Nevertheless, more detailed studies, especially the analysis of sedimentary facies, are needed to verify our inference. As a precaution, those species which may have been reworked were not included in the establishment of the conodont zonation presented herein.

4.3 Change in Conodont Assemblages and Conodont Paleoecology

The change in the composition of conodont faunas may reflect the environmental changes across the Permian-Triassic boundary and in the Early Triassic (Jiang et al., 2007), and the distribution of Triassic conodonts is most likely controlled by paleoenvironmental conditions (Li et al., 2019; Lai and Mei, 2000; Trammer, 1974). Lai and Mei (2000) identified "evolutionary stages" and "events" and considered the evolution of Triassic conodonts to be dominated by an "Extinction-Survival-Recovery Pattern" based on the change of conodont faunas. Narkiewicz and Szulc (2004) and Chen et al. (2019) documented two episodes of conodont faunal change that took place in the Germanic Basin, which were controlled by eustatic sea-level change during the Middle Triassic. At the Shaiwa Section, three successive conodont faunal assemblages can be identified, when reworked specimens are not considered (Fig. 2 and Table 1).

The first assemblage (below Bed 8, Fig. 2) is characterized by a marked abundance of blade-shaped conodonts (*Nicoraella* and *Cratognathus*) and a lack of contemporaneous platform conodonts. In this interval, the blade-shaped conodonts comprise nearly 100% of the collection (except for the four platform elements from Bed 1, Bed 7 and Bed 8). The lack of platform conodonts in the early Anisian has also been identified in the central part of the Germanic Basin by Narkiewicz and Szulc (2004) and Chen et al. (2019). This phenomenon was suggested to be one of most important conodont biogeographical phenomena during the Middle Triassic, in which environmental conditions (more restricted conditions) precluded the development of platform conodonts in the basin (Narkiewicz and Szulc, 2004).

The second assemblage (beds 9–26, Fig. 2) is characterized by the co-existence of blade-shaped and platform conodonts (e.g., *Neogondolella* and *Paragondolella*). The abundance and
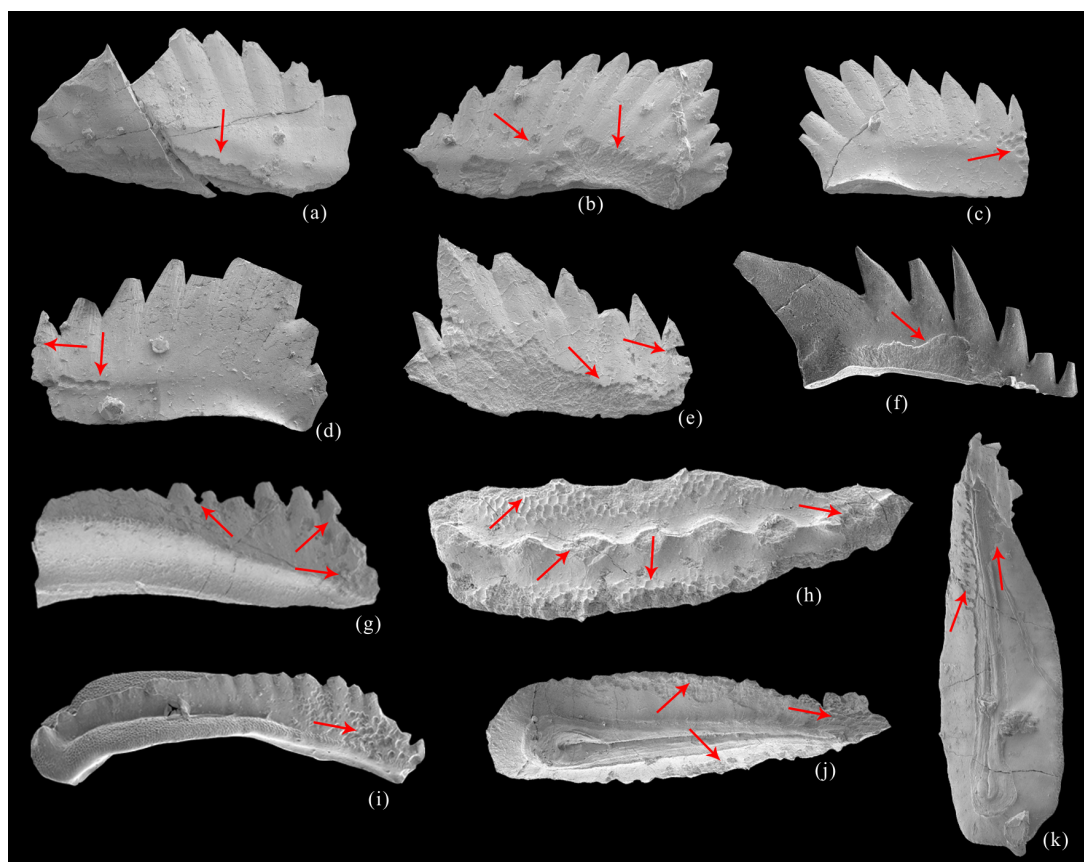

Figure 5. The photographs of abrasion of conodonts surface at the Shaiwa Section. (a)–(e) *Nicoraella* sp.; (f) *Cratognathus* sp.; (g) *Neogondolella* sp.; (h) *Gladigondolella* sp.; (i)–(k) *Paragondolella* sp.; (a) from Bed 1; (b), (c) from Bed 5; (d) from Bed 17; (e) from Bed 2; (f), (g) from Bed 11; (h), (j), (k) from Bed 35; (i) from Bed 26; red arrows show the corrosion of conodonts.

diversity of platform elements increased in this interval. At the Shaiwa Section during this interval, the lithology is mostly dominated by limestone, indicating that the sedimentary environment returned to normal (open) marine conditions (e.g. more oxygenated). The appearance of platform conodont faunas at this time most probably indicates that open marine conditions were likely more suitable for the development of platform conodonts (Narkiewicz and Szulc, 2004).

The third assemblage (beds 27–38, Fig. 2) is marked by the turnover of blade-shaped and platform conodonts. The blade-shaped conodonts, although present in this interval, nevertheless constitute a low percentage of conodont faunas, which are dominated by platform conodonts. This changeover between segminate-dominated and segminiplanate-dominated also occurred during the Early Permian (Sun et al., 2017; Wang et al., 2016) and the Early Triassic (Li et al., 2019; Chen et al., 2015).

Many authors have documented that the segminiplanate conodonts dominated are replaced by the segminate conodonts dominated during the Permian-Triassic transition (e.g., Jiang et al., 2011, 2007; Lai et al., 2001) and the Early Triassic (Chen et al., 2015). In our study, the segminate conodonts dominate below the *Pg. bulgarica* Zone, decline in abundance from Bed 9 to Bed 26 and then are largely replaced by segminiplanate conodonts from Bed 27 to Bed 38 (Fig. 2 and Table 1). This change in the composition of the conodont faunas is probably due to paleoenvironmental change. Indeed, marked lithological change can be observed: the lower part of the section (below the *Pg. bulgarica* Zone) is dominated by clastic rocks intercalated with few carbonate rocks, whereas from Bed 9 to Bed 38 limestone predominates. To date, the ecology of segminiplanate conodonts remains debatable. Orchard (1996) suggested that offshore, deeper, and/or colder marine water environments are more suitable for segminiplanate conodonts. Lai et al. (2001) and Chen et al. (2015) believed that segminiplanate conodonts probably favored oxygenated deeper water habitats. Nicoll et al. (2002) considered that the limpid condition is more suited for segminiplanate conodonts whereas segminate conodonts were adapted to higher levels of turbid water. Li et al. (2019) concluded that temperature was the factor which controlled the distribution and evolution of platform conodonts. Based on the change of lithology at the Shaiwa Section, the depositional environments below the *Pg. bulgarica* Zone probably can be assigned to a restricted shallow marine environment, and segminiplanate conodonts are almost absent in this interval; above this horizon, the environment became more oxygenated and suitable for the conodont animals with segminiplanate elements.

5 CONCLUSIONS

Six conodont zones, the *Nicoraella germanica* Zone, the *Nicoraella kockeli* Zone, the *Paragondolella bulgarica* Zone, the *Neogondolella constricta* Zone, the *Neogondolella cornuta* Zone and the *Paragondolella excelsa* Zone in ascending order, can be established for the Middle Triassic succession at the Shaiwa Section, Guizhou Province, Southwest China. This new investigation promotes a better understanding of the Middle Triassic conodont succession in South China and provides potential local and regional correlation. The Bithynian-Pelsonian boundary is placed at the base of Bed 1 based on the first occurrence of *Ni. kockeli*. The

Pelsonian-Illyrian boundary is marked by the first occurrence of *Ng. constricta* at the lower part of Bed 19. The Anisian-Ladinian boundary is not recognized currently, although the uppermost stratum of the Shaiwa Section could be very close to the base of the Ladinian. The shift in relative abundance between blade-shaped conodonts and platform conodonts, together with lithological changes, indicates that the lower part of the section could be a restricted marine environment that precluded the development of segminiplanate elements, whereas the middle and upper parts of the section were deposited in an oxygenated deeper seawater environment that was more suitable for segminiplanate conodonts.

REFERENCES CITED

Balini, M., Germani, D., Nicora, A., et al., 2000. Ladinian/Carnian Ammonoids and Conodonts from the Classic Schilpario-Pizzo Camino Area (Lombardy): Revaluation of the Biostratigraphic Support to Chronostratigraphy and Paleogeography. *Rivista Italiana di Paleontologia e Stratigrafia*, 106(1): 19–59. https://doi.org/10.13130/2039-4942/5389

Bender, H., 1970. Zur Gliederung der Mediterranen Trias II. Die Conodontenchronologie der Mediterranen Trias. *Extract Annales Géologiques des Pays Helléniques*, 19: 465–540 (in Germany)

Bo, J. F., Yao, J. X., Xiao, J. F., et al., 2017. Seleractinian Coral and Conodont Biostratigraphy of the Middle-Upper Part of the Poduan Formation in Ceheng, Guizhou Province, South China. *Acta Geologica Sinica*, 91(2): 487–497 (in Chinese with English Abstract)

Brack, P., Rieber, H., Nicora, A., et al., 2005. The Global Boundary Stratotype Section and Point (GSSP) of the Ladinian Stage (Middle Triassic) at Bagolino (Southern Alps, Northern Italy) and Its Implications for the Triassic Time Scale. *Episodes*, 28(4): 233–244. https://doi.org/10.18814/epiiugs/2005/v28i4/001

Budurov, K., Stefanov, S., 1973. Etliche neue Plattform-Conodonten aus der Mitteltrias Bulgariens. *Doklady Bolgarskoi Akademii Nauk*, 26(6): 803–806 (in Germany)

Budurov, K., Stefanov, S., 1972. Platform-Condonten und ihre Zonen in der Mittleren Trias Bulgariens. *Mitteilungen Gesell Geologischen Bergbaustud*, 21: 829–863 (in Germany)

Budurov, K., Stefanov, S., 1975. Neue Daten üBer die Conodonten-Chronologie der Balkaniden Mittleren Trias. *Doklady Bolgarskoi Akademii Nauk*, 28(6): 791–794 (in Germany)

Buryi, I. G., 1996. Triassic Conodonts from the Cherts of Nadanhada Range, Northeast China. *Acta Micropalaeontologica Sinica*, 13(2): 207–214 (in Chinese with English Abstract)

Carey, S. P., 1984. Conodont Biofacies of the Triassic of Northwestern Nevada. *Special Paper, Geological Society of America*, 196: 295–306. https://doi.org/10.1130/spe196-p295

Chen, L. D., Wang, C. Y., 2009. Conodont Based Age of the Triassic

Yangliujing Formation in SW Guizhou, China. *Journal of Stratigraphy*, 33(1): 98–103 (in Chinese with English Abstract)

Chen, Y. L., Jiang, H. S., Lai, X. L., et al., 2015. Early Triassic Conodonts of Jiarong, Nanpanjiang Basin, Southern Guizhou Province, South China. *Journal of Asian Earth Sciences*, 105: 104–121. https://doi.org/10.1016/j.jseaes.2015.03.014

Chen, Y. L., Krystyn, L., Orchard, M. J., et al., 2016. A Review of the Evolution, Biostratigraphy, Provincialism and Diversity of Middle and Early Late Triassic Conodonts. *Papers in Palaeontology*, 2(2): 235–263. https://doi.org/10.1002/spp2.1038

Chen, Y. L., Scholze, F., Richoz, S., et al., 2019. Middle Triassic Conodont Assemblages from the Germanic Basin: Implications for Multi-Element Taxonomy and Biogeography. *Journal of Systematic Palaeontology*, 17(5): 359–377. https://doi.org/10.1080/14772019.2018.1424260

Chen, Y., Jiang, H. S., Ogg, J. G., et al., 2020. Early-Middle Triassic Boundary Interval: Integrated Chemo-Bio-Magneto-Stratigraphy of Potential GSSPS for the Base of the Anisian Stage in South China. *Earth and Planetary Science Letters*, 530: 115863. https://doi.org/10.1016/j.epsl.2019.115863

Chen, Z. Q., Benton, M. J., 2012. The Timing and Pattern of Biotic Recovery Following the End-Permian Mass Extinction. *Nature Geoscience*, 5(6): 375–383. https://doi.org/10.1038/ngeo1475

Ding, M. H., Huang, Q. H., 1990. Late Permian-Middle Triassic Conodont Fauna and Paleoecology in Shitouzhai, Ziyun County, Guizhou Province. *Earth Science—Journal of China University of Geosciences*, 15(3): 291–298 (in Chinese with English Abstract)

Dong, Z. Z., Wang, W., 2006. The Conodont Fauna of Yunnan Province. Yunnan Science and Technology Press, Kunming. 128–146 (in Chinese)

Erwin, D. H., Bowring, S. A., Jin, Y. G., 2002. End-Permian Mass Extinctions: A Review. In: Koeberl, C., Macleod, K. G., eds., Catastrophic Events and Mass Extinctions: Impacts and Beyond. *Geological Society of America Special Paper*, 356: 363–383. https://doi.org/10.1130/0-8137-2356-6.363

Escudero-Mozo, M. J., Márquez-Aliaga, A., Goy, A., et al., 2015. Middle Triassic Carbonate Platforms in Eastern Iberia: Evolution of Their Fauna and Palaeogeographic Significance in the Western Tethys. *Palaeogeography*, *Palaeoclimatology*, *Palaeoecology*, 417: 236–260. https://doi.org/10.1016/j.palaeo.2014.10.041

Gao, Y. S., Yang, F. Q., Peng, Y. Q., 2001. Late Permian Deep Water Stratigraphy in Shaiwa of Ziyun, Guizhou. *Journal of Stratigraphy*, 25(2): 116–119 (in Chinese with English Abstract)

Goel, R. K., 1977. Triassic Conodonts from Spiti (Himachal Pradesh), India. *Journal of Paleontology*, 51(6): 1085–1101. https://www.jstor.org/stable/1303823

Golding, M. L., 2018. Reconstruction of the Multielement Apparatus of *Neogondolella* ex gr. *regalis* Mosher, 1970 (Conodonta) from the Anisian (Middle Triassic) in British Columbia, Canada. *Journal of Micropalaeontology*, 37(1): 21–24. https://doi.org/10.5194/jm-37-21-2018

Golding, M. L., Orchard, M. J., 2018. *Magnigondolella*, a New Conodont Genus from the Triassic of North America. *Journal of Paleontology*, 92(2): 207–220. https://doi.org/10.1017/jpa.2017.123

Golding, M. L., Orchard, M. J., 2016. New Species of the Conodont *Neogondolella* from the Anisian (Middle Triassic) of Northeastern British Columbia, Canada, and Their Importance for Regional Correlation. *Journal of Paleontology*, 90(6): 1197–1211. https://doi.org/10.1017/jpa.2016.119

Golding, M. L., Orchard, M. J., Zonneveld, J. P., 2014. A Summary of New Conodont Biostratigraphy and Correlation of the Anisian (Middle Triassic) Strata in British Columbia, Canada. *Albertiana*, 42: 33–40

Goudemand, N., Orchard, M. J., Bucher, H., et al., 2012. The Elusive Origin of *Chiosella timorensis* (Conodont Triassic). *Geobios*, 45(2): 199–207. https://doi.org/10.1016/j.geobios.2011.06.001

Gu, S. Z., Pei, J. C., Yang, F. Q., et al., 2002. Smaller Foraminifera Fauna from the Changxing of the Sidazhai Section, Ziyun County, Southern Guizhou Province. *Acta Micropalaeontologica Sinica*, 19(2): 163–169 (in Chinese with English Abstract)

Hao, W. C., Sun, Y. L., Jiang, D. Y., et al., 2006. Advance in Studies of the Panxian Fauna. *Acta Scientiarum Naturalium Universitatis Pekinensis*, 42(6): 817–823 (in Chinese with English Abstract)

Hornung, T., 2006. Conodont Biostratigraphy of the Lercheck/Königsleiten Section near Berchtesgaden (Late Ladinian-Hallstatt Limestones). *Geo. Alp*, 3: 23–31

Hu, Y. X., Xu, D. L., Tong, J. N., 2006. A Preliminary Study on the Lower Triassic Strata of Sidazhai, Ziyun, Guizhou Province. *Journal of Stratigraphy*, 30(2): 177–182 (in Chinese with English Abstract)

Huang, J. Y., Zhang, K. X., Zhang, Q. Y., et al., 2009. Conodonts Stratigraphy and Sedimentary Environment of the Middle Triassic at Daaozi Section of Luoping County, Yunnan Province, South China. *Acta Micropalaeontologica Sinica*, 26(2): 211–224 (in Chinese with English Abstract)

Huang, J. Y., Zhang, K. X., Zhang, Q. Y., et al., 2011. Advance Research of Conodont Fauna from Shangshikan and Daaozi Sections in Luoping Area, Yunnan Province. *Geological Science and Technology Information*, 30(3): 1–17 (in Chinese with English Abstract)

Huckriede, R., 1958. Die Conodonten der Mediterranen Trias und Ihr Stratigraphischer Wert. *Paläontologische Zeitschrift*, 32(3/4): 141–175 (in Germany)

Ji, Q., Ji, X. X., Feng, H. Z., 2009. Middle Permian Fish Microremains from the Sidazhai Area, Ziyun County, Guizhou Province. *Geological Review*, 55(5): 609–613 (in Chinese with English Abstract)

Ji, W. T., Tong, J. N., Zhao, L. S., et al., 2011. Lower–Middle Triassic Conodont Biostratigraphy of the Qingyan Section, Guizhou Province, Southwest China. *Palaeogeography*, *Palaeoclimatology*, *Palaeoecology*, 308(1/2): 213–223. https://doi.org/10.1016/j.palaeo.2010.08.020

Jiang, H. S., Lai, X. L., Luo, G. M., et al., 2007. Restudy of Conodont Zonation and Evolution across the P/T Boundary at Meishan Section, Changxing, Zhejiang, China. *Global and Planetary Change*, 55(1/2/3): 39–55. https://doi.org/10.1016/j.gloplacha.2006.06.007

Jiang, H. S., Lai, X. L., Yan, C. B., et al., 2011. Revised Conodont Zonation and Conodont Evolution across the Permian-Triassic Boundary at the Shangsi Section, Guangyuan, Sichuan, South China. *Global and Planetary Change*, 77(3/4): 103–115. https://doi.org/10.1016/j.gloplacha.2011.04.003

Koike, T., Igo, H., Takizawa, S., et al., 1971. Contribution to the Geological History of the Japanese Islands by the Conodont Biostratigraphy Part II. *The Journal of the Geological Society of Japan*, 77(3): 165–168. https://doi.org/10.5575/geosoc.77.165

Kovács, S., 1983. On the Evolution of *excelsa*-Stock in the Upper Ladinian-Carnian (Conodonta, Genus Gondolella, Triassic). *Schriftenreihe der Erdwissenschaftlichen Kommissionen*, 5: 107–120

Kovács, S., 1994. Conodonts of Stratigraphical Importance from the Anisian/Ladinian Boundary Interval of the Balaton Highland, Hungary. *Rivista Italiana Di Paleontologia e Stratigrafia*, 99(4): 473–514. https://doi.org/10.13130/2039-4942/8895

Kovács, S., Kozur, H., 1980. Stratigraphische Reichweite der Wichtigsten Conodonten (Ohne Zahnreihenconodonten) der Mittel- und Obertrias. *Geol. Palaont. Mitt. Innsbruck*, 10(2): 47–78 (in Germany)

Kovács, S., Nicora, A., Szabó, I., et al., 1990. Conodont Biostratigraphy of Anisian/Ladinian Boundary Sections in the Balaton Upland (Hungary) and in the Southern Alps (Italy). *Courier Forsch. Inst. Senckenberg*, 188: 171–195

Kozur, H. W., Mostler, H., Krainer, K., 1998. *Sweetospathodus* n. gen. and *Triassospathodus* n. gen., Two Important Lower Triassic Conodont Genera. *Geologia Croatica*, 51(1): 1–5

Kozur, H. W., 2003. Integrated Ammonoid, Conodont and Radiolarian Zonation of the Triassic and some Remarks to Stage/Substage Subdivision and the Numeric Age of the Triassic Stages. *Albertiana*, 28: 57–74

Kozur, H., 1972. Die Conodontengattung Metapolygnathus HAYASHI 1968 und ihr Stratigraphischer Wert. *Geol. Palaont. Mitt. Innsbruck*, 2: 1–37 (in Germany)

Kozur, H., 1989. The Taxonomy of the Gondolellid Conodont in the Permian and Triassic. *Courier Forsch. Inst. Senckenberg*, 117: 409–469

Kozur, H., Krainer, K., Mostler, H., 1994. Middle Triassic Conodonts from the Southern Karawanken Mountains (Southern Alps) and Their Stratigraphic Importance. *Geol. Palaont. Mitt. Innsbruck*, 19: 165–200

Kozur, H., 1993. *Nicoraella postkockeli* n. sp., a New Conodont Species from the Lower Carnian of Hungary. *Neues Jahrbuch für Geologie und Paläontologie-Monatshefte*, 1993(7): 405–412. https://doi.org/10.1127/njgpm/1993/1993/405

Lai, X. L., Mei, S. L., 2000. On Zonation and Evolution of Permian and Triassic Conodonts. Developments in Palaeontology and Stratigraphy. Elsevier, Amsterdam. 371–392. https://doi.org/10.1016/s0920-5446(00)80021-7

Lai, X. L., Wignall, P., Zhang, K. X., 2001. Palaeoecology of the Conodonts *Hindeodus* and *Clarkina* during the Permian-Triassic Transitional Period. *Palaeogeography*, *Palaeoclimatology*, *Palaeoecology*, 171(1/2): 63–72. https://doi.org/10.1016/s0031-0182(01)00269-3

Lehrmann, D. J., Payne, J. L., Felix, S. V., et al., 2003. Permian-Triassic Boundary Sections from Shallow-Marine Carbonate Platforms of the Nanpanjiang Basin, South China: Implications for Oceanic Conditions Associated with the End-Permian Extinction and Its Aftermath. *Palaios*, 18(2): 138–152. https://doi.org/10.1669/0883-1351(2003)18138:pbsfsc>2.0.co;2

Lehrmann, D. J., Payne, J. L., Pei, D. H., et al., 2007. Record of the End-Permian Extinction and Triassic Biotic Recovery in the Chongzuo-Pingguo Platform, Southern Nanpanjiang Basin, Guangxi, South China. *Palaeogeography*, *Palaeoclimatology*, *Palaeoecology*, 252(1/2): 200–217. https://doi.org/10.1016/j.palaeo.2006.11.044

Lehrmann, D. J., Ramezani, J., Bowring, S. A., et al., 2006. Timing of Recovery from the End-Permian Extinction: Geochronologic and Biostratigraphic Constraints from South China. *Geology*, 34(12): 1053. https://doi.org/10.1130/g22827a.1

Lehrmann, D. J., Stepchinski, L., Altiner, D., et al., 2015. An Integrated Biostratigraphy (Conodonts and Foraminifers) and Chronostratigraphy (Paleomagnetic Reversals, Magnetic Susceptibility, Elemental Chemistry, Carbon Isotopes and Geochronology) for the Permian-Upper Triassic Strata of Guandao Section, Nanpanjiang Basin, South China. *Journal of Asian Earth Sciences*, 108: 117–135. https://doi.org/10.1016/j.jseaes.2015.04.030

Li, H. X., Jiang, H. S., Chen, Y. L., et al., 2019. Smithian Platform-Bearing Gondolellid Conodonts from Yiwagou Section, Northwestern China and Implications for Their Geographic Distribution in the Early Triassic. *Journal of Paleontology*, 93(3): 496–511. https://doi.org/10.1017/jpa.2018.93

Li, M. S., Huang, C. J., Hinnov, L., et al., 2018. Astrochronology of the Anisian Stage (Middle Triassic) at the Guandao Reference Section, South China. *Earth and Planetary Science Letters*, 482: 591–606. https://doi.org/10.1016/j.epsl.2017.11.042

Liang, L., Tong, J. N., Song, H. J., et al., 2016. Lower-Middle Triassic Conodont Biostratigraphy of the Mingtang Section, Nanpanjiang Basin, South China. *Palaeogeography*, *Palaeoclimatology*, *Palaeoecology*, 459: 381–393. https://doi.org/10.1016/j.palaeo.2016.07.027

Márquez-Aliaga, A., Valenzuela-Rios, J. I., Calvet, F., et al., 2000. Middle Triassic Conodonts from Northeastern Spain: Biostratigraphic Implications. *Terra Nova*, 12(2): 77–83. https://doi.org/10.1046/j.1365-3121.2000.00273.x

Meco, S., 1999. Conodont Biostratigraphy of Triassic Pelagic Strata, Albania. *Rivista Italiana Di Paleontologia e Stratigrafia*, 105(2): 251–266

Metcalfe, I., 1990. Triassic Conodont Biostratigraphy in the Malay Peninsula. *Geological Society of Malaysia Bulletin*, 26: 133–145. https://doi.org/10.7186/bgsm26199011

Monnet, C., Brack, P., Bucher, H., et al., 2008. Ammonoids of the Middle/Late Anisian Boundary (Middle Triassic) and the Transgression of the Prezzo Limestone in Eastern Lombardy-Giudicarie (Italy). *Swiss Journal of Geosciences*, 101(1): 61–84. https://doi.org/10.1007/s00015-008-1251-7

Mosher, L. C., 1968. Triassic Conodonts from Western North America and Europe and Their Correlation. *Journal of Paleontology*, 42(4): 895–946

Mosher, L. C., Clark, D. L., 1965. Middle Triassic Conodonts from the Prida Formation of Northwestern Nevada. *Journal of Paleontology*, 39(4): 551–565

Muto, S., Takahashi, S., Yamakita, S., et al., 2019. Conodont-Based Age Calibration of the Middle Triassic Anisian Radiolarian Biozones in Pelagic Deep-Sea Bedded Chert. *Bulletin of the Geological Survey of Japan*, 70(1/2): 43–89. https://doi.org/10.9795/bullgsj.70.43

Muttoni, G., Nicora, A., Brack, P., et al., 2004. Integrated Anisian-Ladinian Boundary Chronology. *Palaeogeography*, *Palaeoclimatology*, *Palaeoecology*, 208(1/2): 85–102. https://doi.org/10.1016/j.palaeo.2004.02.030

Narkiewicz, K., 1999. Conodont Biostratigraphy of the Muschelkalk (Middle Triassic) in the Central Part of the Polish Lowlands. *Geological Quarterly*, 43(3): 313–328

Narkiewicz, K., Szulc, J., 2004. Controls on Migration of Conodont Fauna in Peripheral Oceanic Areas: An Example from the Middle Triassic of the Northern Peri-Tethys. *Geobios*, 37(4): 425–436. https://doi.org/10.1016/j.geobios.2003.10.001

Nicoll, R. S., Metcalfe, I., Wang, C. Y., 2002. New Species of the Conodont Genus *Hindeodus* and the Conodont Biostratigraphy of the Permian-Triassic Boundary Interval. *Journal of Asian Earth Sciences*, 20(6): 609–631. https://doi.org/10.1016/s1367-9120(02)00021-4

Nicora, A., 1977. Lower Anisian Platform-Conodonts from the Tethys and Nevada: Taxonomic and Stratigraphic Revision. *Palaeontographica Abteilung A*, 157: 88–107

Nogami, Y., 1968. Trias-Conodonten von Timor, Malaysien und Japan (Palaeontological Study of Portuguese Timor, 5) Memoirs of the Faculty of Science, Kyoto University. *Series of Geology and Mineralogy*, 36: 115–135 (in Germany)

Ogg, G. J., Huang, C. J., Hinnov, L., 2014. Triassic Timescale Status: A Brief Overview. *Albertiana*, 41: 3–30

Ogg, J. G., Ogg, G. M., Gradstein, F. M., 2016. Triassic: A Concise Geologic Time Scale. Elsevier, Amsterdam. 133–149. https://doi.org/10.1016/b978-0-444-59467-9.00011-x

Orchard, M. J., 1995. Taxonomy and Correlation of Lower Triassic (Spathian) Segminate Conodonts from Oman and Revision of some Species of *Neospathodus*. *Journal of Paleontology*, 69(1): 110–122. https://doi.org/10.1017/s0022336000026962

Orchard, M. J., 2005. Multielement Conodont Apparatuses of Triassic Gondolelloidea. *Special Papers in Palaeontology*, 73: 73–101

Orchard, M. J., 2010. Triassic Conodonts and Their Role in Stage Boundary Definition. *Geological Society*, *London*, *Special Publications*, 334(1): 139–161. https://doi.org/10.1144/sp334.7

Orchard, M. J., 1996. Conodont Fauna from the Permian-Triassic Boundary: Observations and Reservations. *Permophiles*, 28: 29–35

Orchard, M. J., Gradinaru, E., Nicora, A., 2007a. A Summary of the Conodont Succession around the Olenekian-Anisian Boundary at Deşli Caira, North Dobrogea, Romania. In: Lucas, S. G., Spielmann, J. A., eds., The Global Triassic. *Mexico Museum of Natural History and Science Bulletin*, 41: 341–346

Orchard, M. J., Lehrmann, D., Wei, J. Y., et al., 2007b. Conodonts from the Olenekian-Anisian Boundary Beds, Guandao, Guizhou Province, China. In: Lucas, S. G., Spielmann, J. A., eds., The Global Triassic. *New Mexico Museum of Natural History and Science Bulletin*, 41: 347–354

Orchard, M. J., Tozer, E. T., 1997. Triassic Conodont Biochronology, Its Calibration with the Ammonoid Standard, and a Biostratigraphic Summary for the Western Canada Sedimentary Basin. *Bulletin of Canadian Petroleum Geology*, 45(4): 675–692

Ovtcharova, M., Goudemand, N., Hammer, Ø., et al., 2015. Developing a Strategy for Accurate Definition of a Geological Boundary through Radio-Isotopic and Biochronological Dating: The Early-Middle Triassic Boundary (South China). *Earth-Science Reviews*, 146: 65–76. https://doi.org/10.1016/j.earscirev.2015.03.006

Payne, J. L., Lehrmann, D. J., Wei, J. Y., et al., 2006. The Pattern and Timing of Biotic Recovery from the End-Permian Extinction on the Great Bank of Guizhou, Guizhou Province, China. *Palaios*, 21(1): 63–85. https://doi.org/10.2110/palo.2005.p05-12p

Payne, J. L., Lehrmann, D. J., Wei, J. Y., et al., 2004. Large Perturbations of the Carbon Cycle during Recovery from the End-Permian Extinction. *Science*, 305(5683): 506–509. https://doi.org/10.1126/science.1097023

Qin, D. X., Yan, C. X., Xiong, J. F., 1993. New Advance in the Biostratigraphy of Triassic Conodonts in Central Guizhou. *Geology of Guizhou*, 10(2): 120–130 (in Chinese with English Abstract)

Rao, R. B., Zhu, Z. X., Huang, S. B., 1985. Fossil Bivavia and Conodonts from Middle Triassic Ladinic Stage in Songpan County, Western Sichuan. *Contribution to the Geology of the Qinghai-Xizang* (*Tibet*) *Plateau*, 9: 199–205

Sepkoski, J. J. Jr., 1984. A Kinetic Model of Phanerozoic Taxonomic Diversity. III. Post-Paleozoic Families and Mass Extinctions. *Paleobiology*, 10(2): 246–267. https://doi.org/10.1017/s0094837300008186

Song, H. J., Wignall, P. B., Chen, Z. Q., et al., 2011. Recovery Tempo and Pattern of Marine Ecosystems after the End-Permian Mass Extinction. *Geology*, 39(8): 739–742. https://doi.org/10.1130/g32191.1

Song, H. J., Wignall, P. B., Tong, J. N., et al., 2012. Geochemical Evidence from Bio-Apatite for Multiple Oceanic Anoxic Events during Permian-Triassic Transition and the Link with End-Permian Extinction and Recovery. *Earth and Planetary Science Letters*, 353/354: 12–21. https://doi.org/10.1016/j.epsl.2012.07.005

Song, H. J., Wignall, P. B., Tong, J. N., et al., 2015. Integrated Sr Isotope Variations and Global Environmental Changes through the Late Permian to Early Late Triassic. *Earth and Planetary Science Letters*, 424: 140–147. https://doi.org/10.1016/j.epsl.2015.05.035

Song, H. Y., Tong, J. N., Algeo, T. J., et al., 2013. Large Vertical $\delta^{13}C_{DIC}$ Gradients in Early Triassic Seas of the South China Craton: Implications for Oceanographic Changes Related to Siberian Traps Volcanism. *Global and Planetary Change*, 105: 7–20. https://doi.org/10.1016/j.gloplacha.2012.10.023

Sudar, M. N., Budurov, K., 1979. New Conodonts from the Triassic in Yugoslavia and Bulgaria. *Geologica Balcanica*, 9(3): 47–52

Sun, Y. D., Liu, X. T., Yan, J. X., et al., 2017. Permian (Artinskian to Wuchapingian) Conodont Biostratigraphy in the Tieqiao Section, Laibin Area, South China. *Palaeogeography, Palaeoclimatology, Palaeoecology*, 465: 42–63. https://doi.org/10.1016/j.palaeo.2016.10.013

Sun, Y., Joachimski, M. M., Wignall, P. B., et al., 2012. Lethally Hot Temperatures during the Early Triassic Greenhouse. *Science*, 338(6105): 366–370. https://doi.org/10.1126/science.1224126

Sun, Z. Y., Hao, W. C., Sun, Y. L., et al., 2009. The Conodont Genus *Nicoraella* and a New Species from the Anisian of Guizhou, South China. *Neues Jahrbuch für Geologie und Paläontologie—Abhandlungen*, 252(2): 227–235. https://doi.org/10.1127/0077-7749/2009/0252-0227

Sun, Z. Y., Jiang, D. Y., Sun, Y. L., et al., 2014. Conodont Biostratigraphy of the Upper Member of the Guanling Formation in Yangjuan-Chupiwa Section, Guizhou Province, South China. *Acta Scientiarum Naturalium Universitatis Pekinensis*, 50(2): 269–280 (in Chinese with English Abstract)

Sun, Z. Y., Hao, W. C., Sun, Y. L., et al., 2006. Conodont Evidence for the Age of the Panxian Fauna, Guizhou, China. *Acta Geologica Sinica*, 80(5): 621–630. https://doi.org/10.111/j.1755-6724.2006.tb00284.x

Sweet, W. C., 1970. Uppermost Permian and Lower Triassic Conodonts of the Salt Range and Trans-Indus Ranges, West Pakistan. *University of Kansas, Department of Geology Special Publications*, 4: 207–275

Tatge, U., 1956. Conodonten Aus Dem Germanischen Muschelkalk. *Paläontologische Zeitschrift*, 30(3/4): 129–147. https://doi.org/10.1007/bf03041777

Tian, C. R., 1983. The Triassic Conodonts from Tulong Village, Nyalam County, Tibet. *Geological Review*, 29(5): 153–165 (in Chinese with English Abstract)

Tong, J. N., Chu, D. L., Liang, L., et al., 2019. Triassic Integrative Stratigraphy and Timescale of China. *Science China Earth Sciences*, 62(1): 189–222. https://doi.org/10.1007/s11430-018-9278-0

Trammer, J., 1971. Middle Triassic (Muschelkalk) Conodonts from the SW Margin of the Holy Cross Mts. *Acta Geologica Polonica*, 21(3): 379–386

Trammer, J., 1972. Stratigraphical and Paleogeographical Significance of Conodonts from the Muschelkalk of the Holy Cross Mts. *Acta Palaeontologica Polonica*, 22(2): 219–232

Trammer, J., 1974. Evolutionary Trends and Pattern of Extinction of Triassic Conodonts. *Acta Palaeontologica Polonica*, 19(2): 251–264

Trammer, J., 1975. Stratigraphy and Facies Development of the Muschelkalk in the South-Western Holy Cross Mts. *Acta Geologica Polonica*, 25(2): 179–216

Vörös, A., 2003. The Pelsonian Substage on the Balaton Highland (Middle Triassic, Hungary). *Geologica Hungarica, Series Palaeontologica*, 55: 159–177

Wang, C. Y., 1991. Triassic Conodont Biostratigraphy of China. *Journal of Stratigraphy*, 15(4): 311–312 (in Chinese with English Abstract)

Wang, C. Y., Wang, Z. H., 1976. Triassic Conodonts in the Mount Jolmo Lungma Region. In: Xizang Scientific Expedition Work-Team of Chinese Academy of Sciences, ed., A Report of Scientific Expedition in the Mount Jolmo Lungma Region 1966–1968 (Paleontology). Science Press, Beijing. 387–416 (in Chinese)

Wang, D. C., Jiang, H. S., Gu, S. Z., et al., 2016. Cisuralian-Guadalupian Conodont Sequence from the Shaiwa Section, Ziyun, Guizhou, South China. *Palaeogeography, Palaeoclimatology, Palaeoecology*, 457: 1–22. https://doi.org/10.1016/j.palaeo.2016.05.030

Wang, H. M., 1996. Discovery of Conodonts in Xinyuan Formation of Middle Triassic of Mengjiang in Luodian County, Guizhou and Its Stratigraphic Significance. *Guizhou Geology*, 13(3): 220–224 (in Chinese with English Abstract)

Wang, H. M., Wang, X. L., Li, R. X., et al., 2005. Triassic Conodont Suc-

cession and Stage Subdivision of the Guandao Section, Luodian, Guizhou. *Acta Palaeontologica Sinica*, 44(4): 611–626 (in Chinese with English Abstract)

Wang, X. Q., Shi, X. Y., 2008. Sedimentary Characteristics and Evolution of the Late Paleozoic Leye Isolated Carbonate Platform in Northwest Guangxi. *Journal of Palaeogeography*, 10(4): 329–340 (in Chinese with English Abstract)

Wang, Z. H., Dai, J. Y., 1981. Triassic Conodont from the Jiangyou-Beichuan Area, Sichuan Province. *Acta Palaeontologica Sinica*, 20(2): 138–152 (in Chinese with English Abstract)

Wang, Z. H., Zhong, D., 1994. Triassic Conodonts from Different Facies in Eastern Yunnan, Western Guizhou and Northern Guangxi. *Acta Micropalaeontologica Sinica*, 11(4): 379–412 (in Chinese with English Abstract)

Wu, G. C., Ji, Z. S., Liao, W. H., et al., 2019. New Biostratigraphic Evidence of Late Permian to Late Triassic Deposits from Central Tibet and Their Paleogeographic Implications. *Lithosphere*, 11(5): 683–696. https://doi.org/10.1130/l1046.1

Wu, G. C., Yao, J. X., Ji, Z. S., et al., 2008. Discovery of the Upper Qingyanian Conodonts in the Qingyan Cross-Section of Guizhou and Its Significance. *Acta Geologica Sinica*, 82(2): 145–154 (in Chinese with English Abstract)

Wu, G. C., Yao, J. X., Ji, Z. S., 2007. Triassic Conodont Biostratigraphy in the Coqên Area, Western Gangdise, Tibet, China. *Geological Bulletin of China*, 26(8): 938–946 (in Chinese with English Abstract)

Wu, H. R., 2003. Discussion on Tectonic Palaeogeography of Nanpanjiang Sea in the Late Palaeozoic and Triassic. *Journal of Palaeogeography*, 5(1): 63–76 (in Chinese with English Abstract)

Xie, T., Liu, S. L., Lou, X. Y., et al., 2019. Discovery and Significance of the Conodonts (Anisian, Middle Triassic) from Pojiao Section in Anlong Area, Guizhou Province. *Geological Review*, 65(2): 280–288 (in Chinese with English Abstract)

Yan, C. B., Jiang, H. S., Lai, X. L., et al., 2015. The Relationship between the "Green-Bean Rock" Layers and Conodont *Chiosella timorensis* and Implications on Defining the Early-Middle Triassic Boundary in the Nanpanjiang Basin, South China. *Journal of Earth Science*, 26(2): 236–245. https://doi.org/10.1007/s12583-015-0535-x

Yang, F. Q., Gao, Y. Q., 2000. Late Permian Deep Water Strata and Bivalves of South Guizhou. *Geoscience*, 14(3): 327–332 (in Chinese with English Abstract)

Yang, S. R., Hao, W. C., Wang, X. P., 1999. Triassic Conodont Secquences

from Different Facies in China. In: Yao, A., Ezaki, Y., Hao, W. C., et al., eds., Biotic and Geological Development of the Paleo-Tethys in China. Peking University Press, Beijing. 97–112 (in Chinese)

Yang, S. R., Wang, X. P., Hao, W. C., 1986. Early and Middle Triassic Conodonts Sequence in Western Guangxi. *Acta Scientiarum Naturalium Universitatis Pekinensis*, 22(4): 90–106 (in Chinese with English Abstract)

Yao, J. X., Ji, Z. S., Wang, L. T., et al., 2004. Research on Conodont Biostratigraphy near the Bottom Boundary of the Middle Triassic Qingyan Stage in the Southern Guizhou Province. *Acta Geologica Sinica*, 78(5): 577–585 (in Chinese with English Abstract)

Yuan, A. H., Sylvie, C., Feng, Q. L., et al., 2009. Ostracods from the Uppermost Permian Siliceous and Muddy Rocks of Guizhou and Anhui. *Acta Micropalaeontologica Sinica*, 26(4): 385–403 (in Chinese with English Abstract)

Yuan, J. L., Jiang, H. S., Wang, D. C., 2015. LST: A New Inorganic Heavy Liquid Used in Conodont Separation. *Geological Science and Technology Information*, 34(5): 230–235 (in Chinese with English Abstract)

Zawidzka, K., 1975. Conodont Stratigraphy and Sedimentary Environment of the Muschelkalk in Upper Silesia. *Acta Geologica Polonica*, 25(2): 217–257

Zhang, L., Orchard, M. J., Algeo, T. J., et al., 2019. An Intercalibrated Triassic Conodont Succession and Carbonate Carbon Isotope Profile, Kamura, Japan. *Palaeogeography, Palaeoclimatology, Palaeoecology*, 519: 65–83. https://doi.org/10.1016/j.palaeo.2017.09.001

Zhang, Q. Y., Zhou, C. Y., Lu, T., et al., 2009. A Conodont-Based Middle Triassic Age Assignment for the Luoping Biota of Yunnan, China. *Science in China Series D: Earth Sciences*, 52(10): 1673–1678. https://doi.org/10.1007/s11430-009-0114-z

Zhang, Z. T., Sun, Y. D., Lai, X. L., et al., 2017. Early Carnian Conodont Fauna at Yongyue, Zhenfeng Area and Its Implication for Ladinian-Carnian Subdivision in Guizhou, South China. *Palaeogeography, Palaeoclimatology, Palaeoecology*, 486: 142–157. https://doi.org/10.1016/j.palaeo.2017.02.011

Zhao, X. W., Zhang, K. X., 1991. Triassci Conodonts from the Ngari Area, Xizang (Tibet), China. *Acta Micropalaeontologica Sinica*, 8(4): 433–440 (in Chinese with English Abstract)

Zhou, G. F., Mao, Q., Chen, Y. M., et al., 2006. A Research into Triassic Biostratigraphy of the Qomolongma Area in South Xizang (Tibet). *Geological Review*, 52(3): 386–395 (in Chinese with English Abstract)
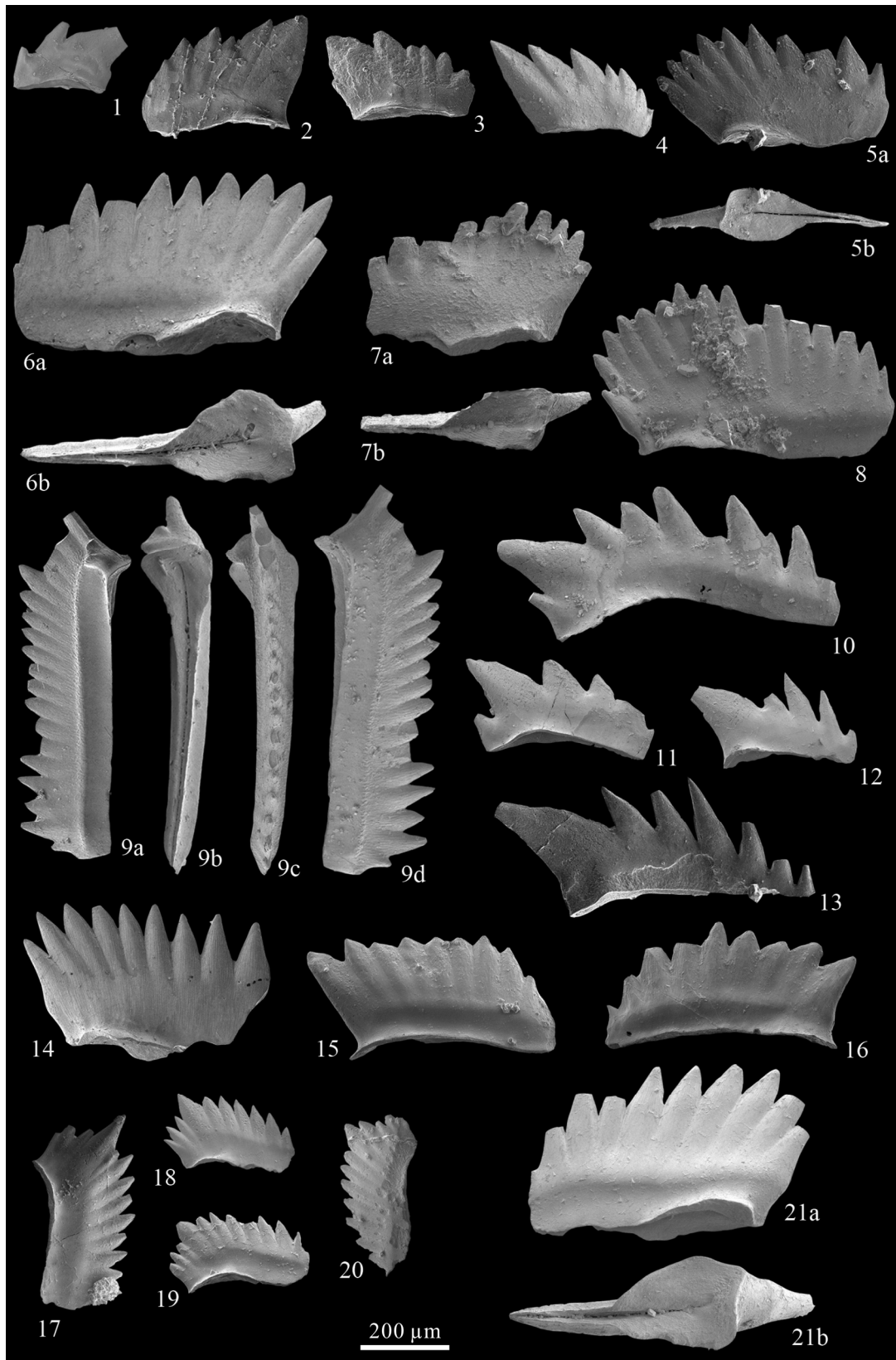
Plate 1. SEM photographs of the key conodont elements from the Shaiwa Section. 1. *Spathicuspus spathi* (Sweet, 1970), from Bed 1; 2, 4. *Nicoraella* sp., 2 from Bed 7, 4 from Bed 19; 3. *Nicoraella* cf. *kockeli* (Tatge, 1956), from Bed 11; 5, 6, 21. *Triassospathodus symmetricus* (Orchard, 1995), 5, 6 from Bed 11, 21 from Bed 2; 5a, 6a, 21a lateral view; 5b, 6c, 21b lower view; 7, 8. *Neospathodus homeri* (Bender, 1970), from Bed 4; 7a, 8 lateral view; 7b lower view; 9. *Chiosella timorensis* (Nogami, 1968), from Bed 11; 9a, 9d lateral view; 9b lower view; 9c upper view; 10, 11. *Cratognathus kochi* (Huckriede, 1958), 10 from Bed 11; 11 from Bed 5; 12, 13. *Cratognathus* sp., 12 from Bed 5, 13 from Bed 11; 14. *Triassospathodus* sp., from Bed 11; 15, 16. *Neospathodus excelsus* (Wang and Wang, 1976), 15 from Bed 9, 16 from Bed 11; 17–20. *Nicoraella microdus* (Mosher, 1968), 17, 18, 20 from Bed 5, 19 from Bed 6.
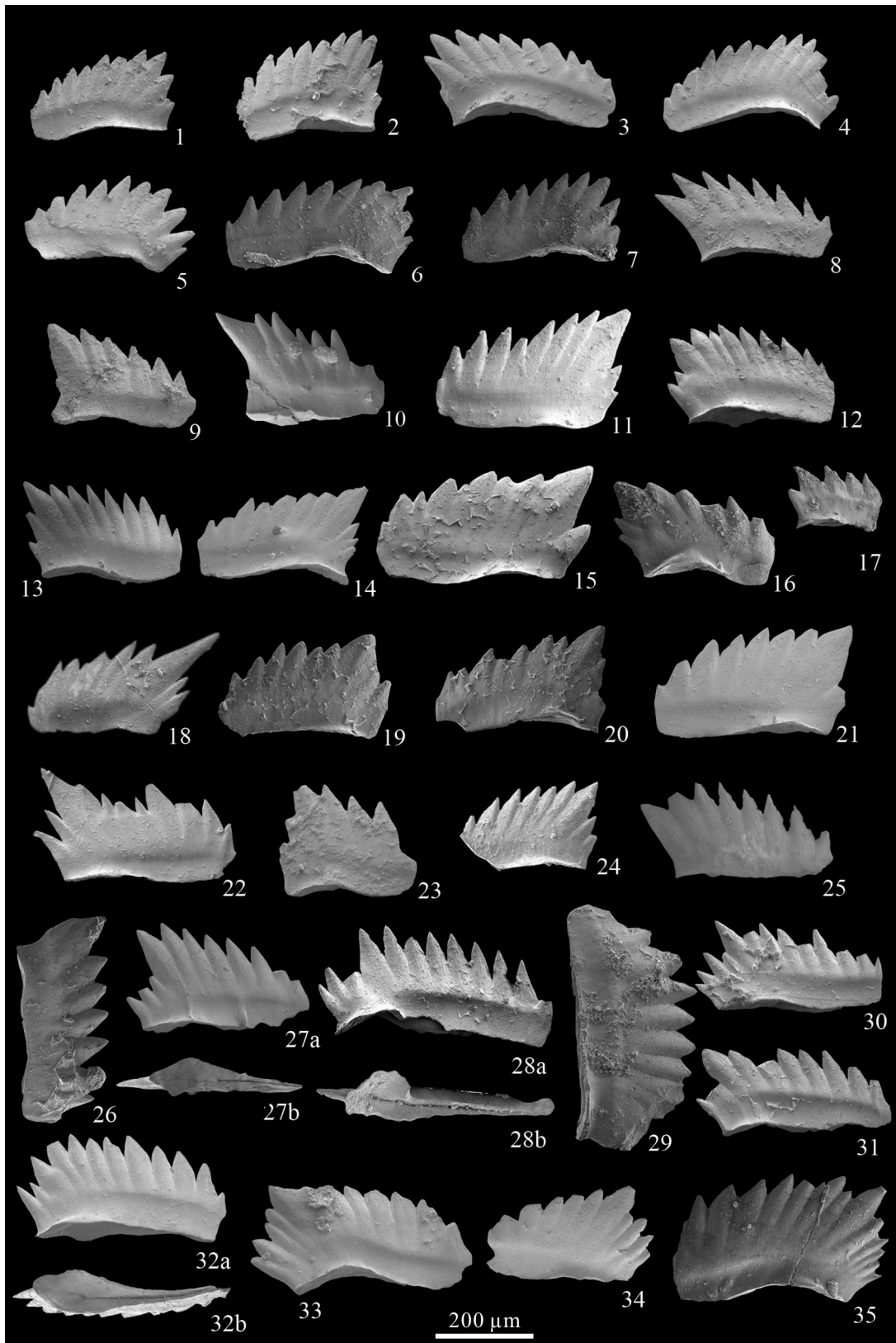
Plate 2. SEM photographs of the key conodont elements from the Shaiwa Section. 1–8. *Nicoraella germanica* (Kozur, 1972), 1, 2, 3, 4 from Bed 19, 5, 8 from Bed 2, 6, 7 from Bed 26; 9, 10. *Nicoraella parabudaensis* (Sun et al., 2009), 9 from Bed 5, 10 from Bed 35; 11–24. *Nicoraella kockeli* (Tatge, 1956), 11, 13, 14 from Bed 35, 12, 21, 22 from Bed 2, 15, 19, 20 from Bed 19, 16 from Bed 26, 17 from Bed 1, 18, 23 from Bed 5, 24 from Bed 38; 25, 26. *Chiosella* n. sp. A (Orchard et al., 2007b), 25 from Bed N6, 26 from Bed 10; 27. *Nicoraella* sp., from Bed 5; 27a lateral view; 27b lower view; 28–31. *Chiosella* sp., 28 from Bed 19, 29 from Bed 9, 30, 31 from Bed 2; 28a, 29, 30, 31 lateral view; 28b lower view; 32. *Neospathodus* sp., from Bed 2; 32a lateral view; 32b lower view; 33–35. *Nicoraella* aff. *microdus* (Mosher, 1968), 33, 34 from Bed 5, 35 from Bed 26.

Plate 3. SEM photographs of the key conodont elements from the Shaiwa Section. 1, 2. *Chiosella timorensis* (Nogami, 1968), 1 from Bed 7, 2 from Bed 20; 1a, 1d, 2a, 2d lateral view; 1b, 2c upper view; 1c, 2b lower view; 3, 4. *Neogondolella cornuta* (Budurov and Stefanov, 1972), 3, 4 from Bed 33; 3a, 4a, upper view; 3b, 4b, lateral view; 3c, 4c, lower view; 5, 6. *Neogondolella longa* (Budurov and Stefanov, 1973), 5 from Bed 33, 6 from Bed 35; 5a, 6a upper view; 5b, 6b lateral view; 5c, 6c lower view; 7. *Magnigondolella julii* (Golding and Orchard, 2018), from Bed 10; 7a upper view; 7b lateral view; 7c lower view; 8, 9. *Magnigondolella* sp., 8 from Bed 33; 9 from Bed 26; 8a, 9a upper view; 8b, 9b lateral view; 8c, 9c lower view; 10. *Magnigondolella* sp., from Bed 26; 10a upper view; 10b lateral view; 11. *Magnigondolella dilacerata* (Golding and Orchard, 2016), from Bed 24; 11a upper view; 11b lateral view; 11c lower view.
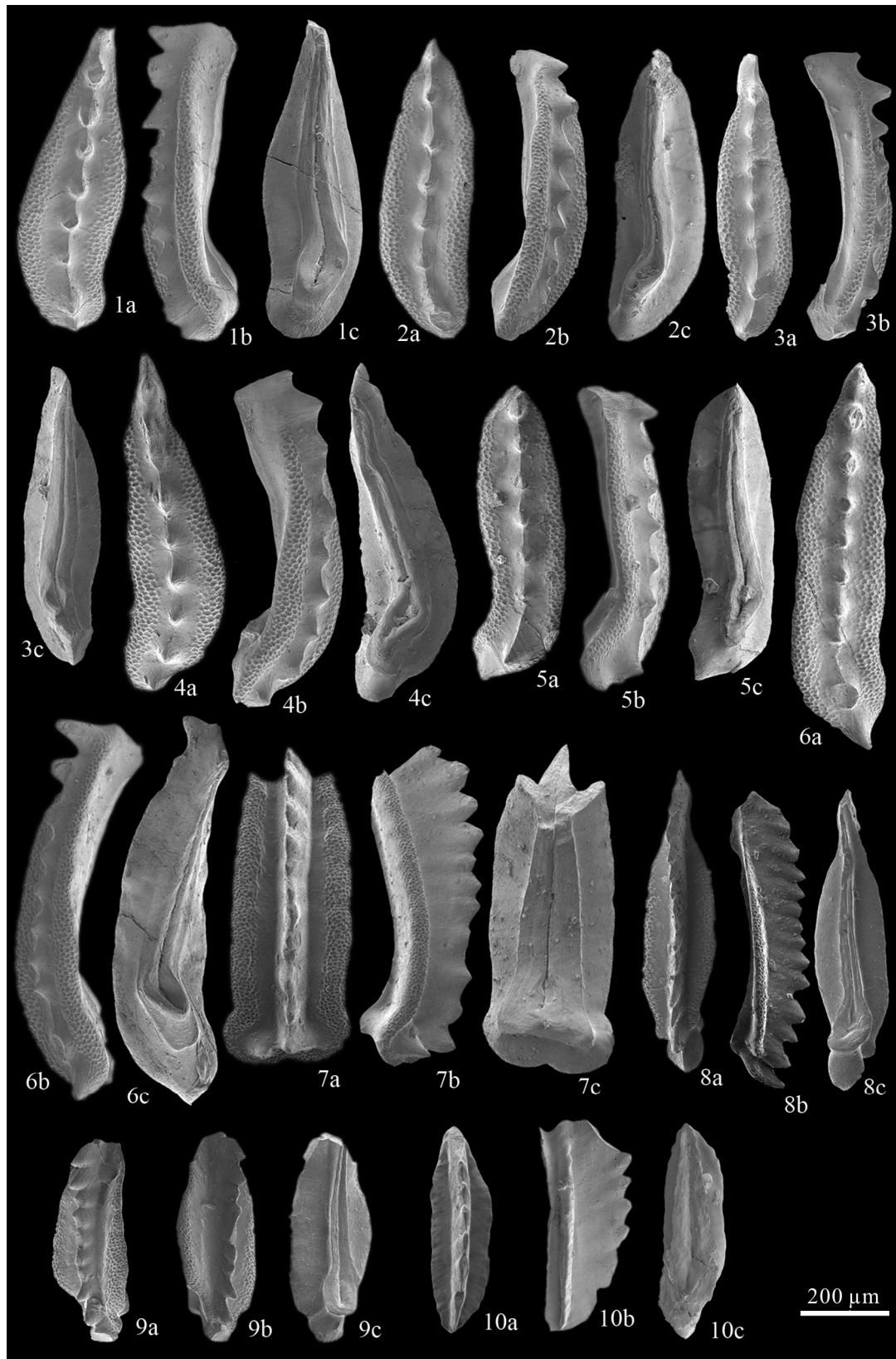
Plate 4. SEM photographs of the key conodont elements from the Shaiwa Section. 1–5. *Gladigondolella budurovi* (Kovács and Kozur, 1980): 1, 2, 3, 5 from Bed 35, 4 from Bed 36; 1a–5a upper view; 1b–5b lateral view; 1c–5c lower view; 6. *Gladigondolella malayensis* (Nogami, 1968), from Bed 35; 6a upper view; 6b lateral view; 6c lower view; 7. *Paragondolella bifurcata* (Budurov and Stefanov, 1972), from Bed 9; 7a upper view; 7b lateral view; 7c lower view; 8. *Magnigondolella julii* (Golding and Orchard, 2018), from Bed 20; 8a upper view; 8b lateral view; 8c lower view; 9. *Neogondolella* sp., from Bed 24; 9a upper view; 9b lateral view; 9c lower view; 10. *Paragondolella* sp., from Bed 1; 10a upper view; 10b lateral view; 10c lower view.

Plate 5. SEM photographs of the key conodont elements from the Shaiwa Section. 1, 2. *Paragondolella bulgarica* (Budurov and Stefanov, 1972), 1, 2 from Bed 11; 1a, 2a upper view; 1b, 2b lateral view; 1c, 2c lower view; 3–5, 8. *Paragondolella bifurcata* (Budurov and Stefanov, 1972), 3 from Bed 11, 4 from Bed 20, 5 from Bed 35, 8 from Bed 20; 3a–5a, 8a upper view; 3b–5b, 8b lateral view; 3c–5c, 8c lower view; 6, 10. *Paragondolella* cf. *bifurcata* (Budurov and Stefanov, 1972), 6, 10 from Bed 20; 6a, 10a upper view; 6b, 10b lateral view; 6c, 10c lower view; 7. *Paragondolella* cf. *tornaensis* (Kovács, 1983), from Bed 35; 7a upper view; 7b lateral view; 10c lower view; 9. *Paragondolella* cf. *liebermani* (Kovács and Krystyn in Kovács, 1994), from Bed 35; 9a upper view; 9b lateral view; 9c lower view; 11. *Paragondolella* sp., from Bed 20; 11a upper view; 11b lateral view; 11c lower view.

Plate 6. SEM photographs of the key conodont elements from the Shaiwa Section. 1, 2. *Paragondolella* cf. *bifurcata* (Budurov and Stefanov, 1972), 1 from Bed 36, 2 from Bed 9; 1a, 2a upper view; 1b, 2b lateral view; 1c, 2c lower view; 3. *Paragondolella* cf. *tornaensis* (Kovács, 1983), from Bed 35; 3a upper view; 3b lateral view; 3c lower view; 4, 5. *Paragondolella tornaensis* (Kovács, 1983), from Bed 35; 4a, 5a upper view; 4b, 5b lateral view; 4c, 5c lower view; 8, 10, 11. *Magnigondolella* sp., from Bed 11; 8a, 10a, 11a upper view; 8b, 10b,11b lateral view; 8c, 10c, 11c lower view; 6, 7. *Neogondolella* sp., 6 from bed 11, 7 from Bed 35; 6a, 7a upper view; 6b, 7b lateral view; 6c, 7c lower view; 9. *Magnigondolella* cf. *julii* (Golding and Orchard, 2018), from Bed 11; 9a upper view; 9b lateral view; 9c lower view; 12. *Magnigondolella dilacerata* (Golding and Orchard, 2016), from Bed 11; 12a upper view; 12b lateral view; 12c lower view.
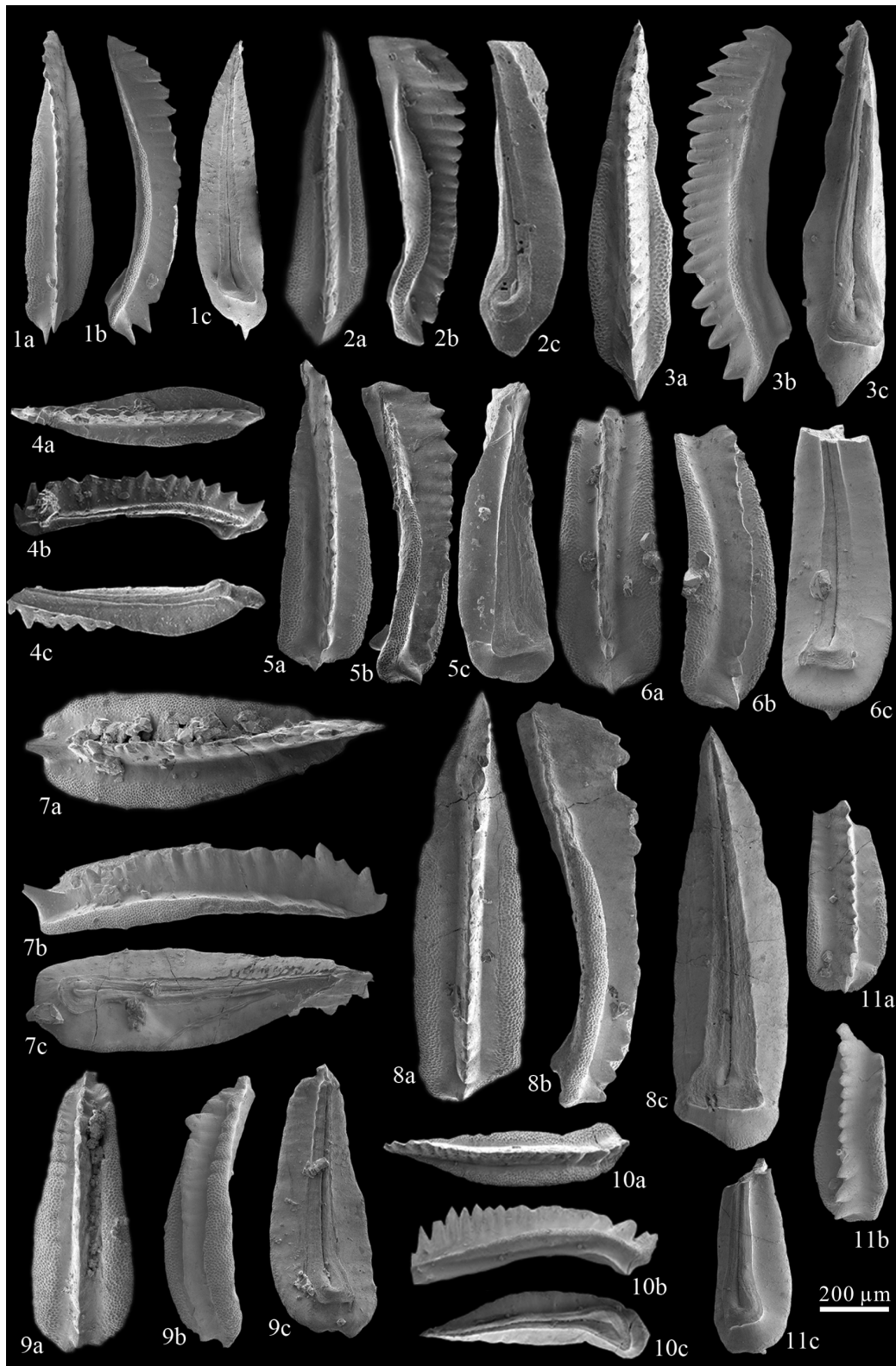
Plate 7. SEM photographs of the key conodont elements from the Shaiwa Section. 1, 10. *Magnigondolella dilacerata* (Golding and Orchard, 2016), 1 from Bed 19; 10 from Bed 35; 1a, 10a upper view; 1b, 10b lateral view; 1c, 10c lower view; 2. *Neogondolella* cf. *cornuta* (Budurov and Stefanov, 1972), from Bed 26; 2a upper view; 2b lateral view; 2c lower view; 3. *Paragondolella bulgarica* (Budurov and Stefanov, 1972), from Bed 35; 3a upper view; 3b lateral view, 3c lower view; 4. *Neogondolella cornuta* (Budurov and Stefanov, 1972), from Bed 33; 4a upper view; 4b lateral view; 4c lower view; 5, 6. *Paragondolella hanbulogi* (Sudar and Budurov, 1979), 5 from Bed 20; 6 from Bed 9; 5a, 6a upper view; 5b, 6b lateral view; 5c, 6c lower view; 7. *Paragondolella* cf. *tornaensis* (Kovács, 1983), from Bed 36; 7a upper view; 7b lateral view; 7c lower view; 8. *Paragondolella* cf. *bifurcata* (Budurov and Stefanov, 1972), from Bed 11; 8a upper view; 8b lateral view; 8c lower view; 9. *Paragondolella tornaensis* (Kovács, 1983), from Bed 35; 9a upper view; 9b lateral view; 9c lower view; 11. *Paragondolella excelsa* (Mosher, 1968), from Bed 35; 11a upper view; 11b lateral view; 11c lower view.
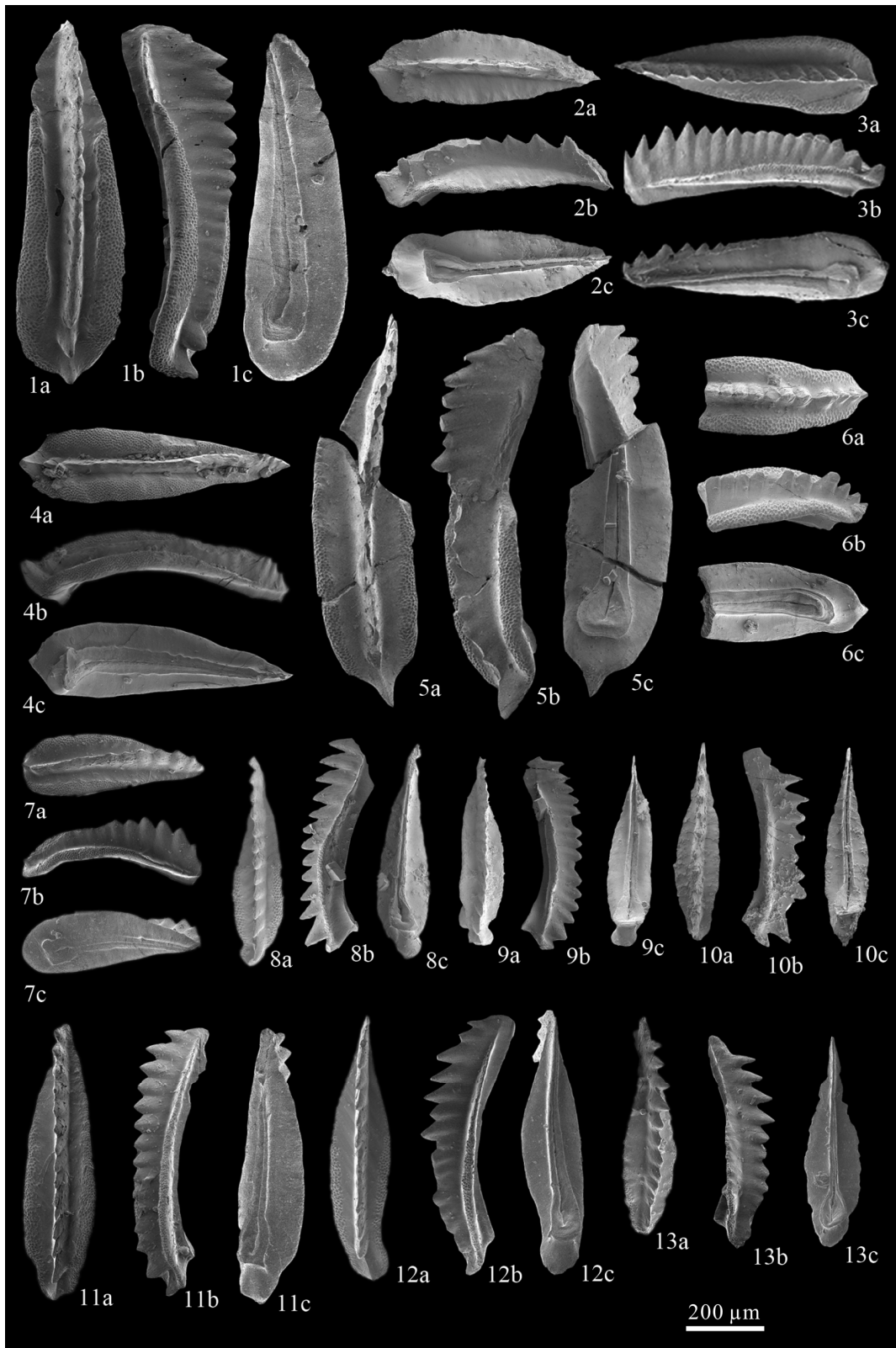
Plate 8. SEM photographs of the key conodont elements from the Shaiwa Section. 1, 3. *Paragondolella* cf. *bifurcata* (Budurov and Stefanov, 1972), 1 from Bed 26, 3 from Bed 11; 1a, 3a upper view; 1b, 3b lateral view; 1c, 3c lower view. 4. *Paragondolella bifurcata* (Budurov and Stefanov, 1972), from Bed 36; 4a upper view; 4b lateral view; 4c lower view. 2. *Neogondolella curva* (Golding and Orchard, 2016), 2 from Bed 19; 2a upper view; 2b lateral view; 2c lower view; 5. *Paragondolella bulgarica* (Budurov and Stefanov, 1972), from Bed 11; 5a upper view; 5b lateral view; 5c lower view; 6. *Neogondolella* cf. *tenera* (Golding and Orchard, 2016), from Bed 35; 6a upper view; 6b lateral view; 6c lower view; 7. *Paragondolella* sp., from Bed 21; 7a upper view; 7b lateral view; 7c lower view; 8–13. *Neogondolella constricta* (Mosher and Clark, 1965), 8, 9 from Bed 35, 10 from Bed 19, 11 from Bed 24; 12, 13 from Bed 20; 8a–13a upper view; 8b–13b lateral view; 8c–13c lower view.
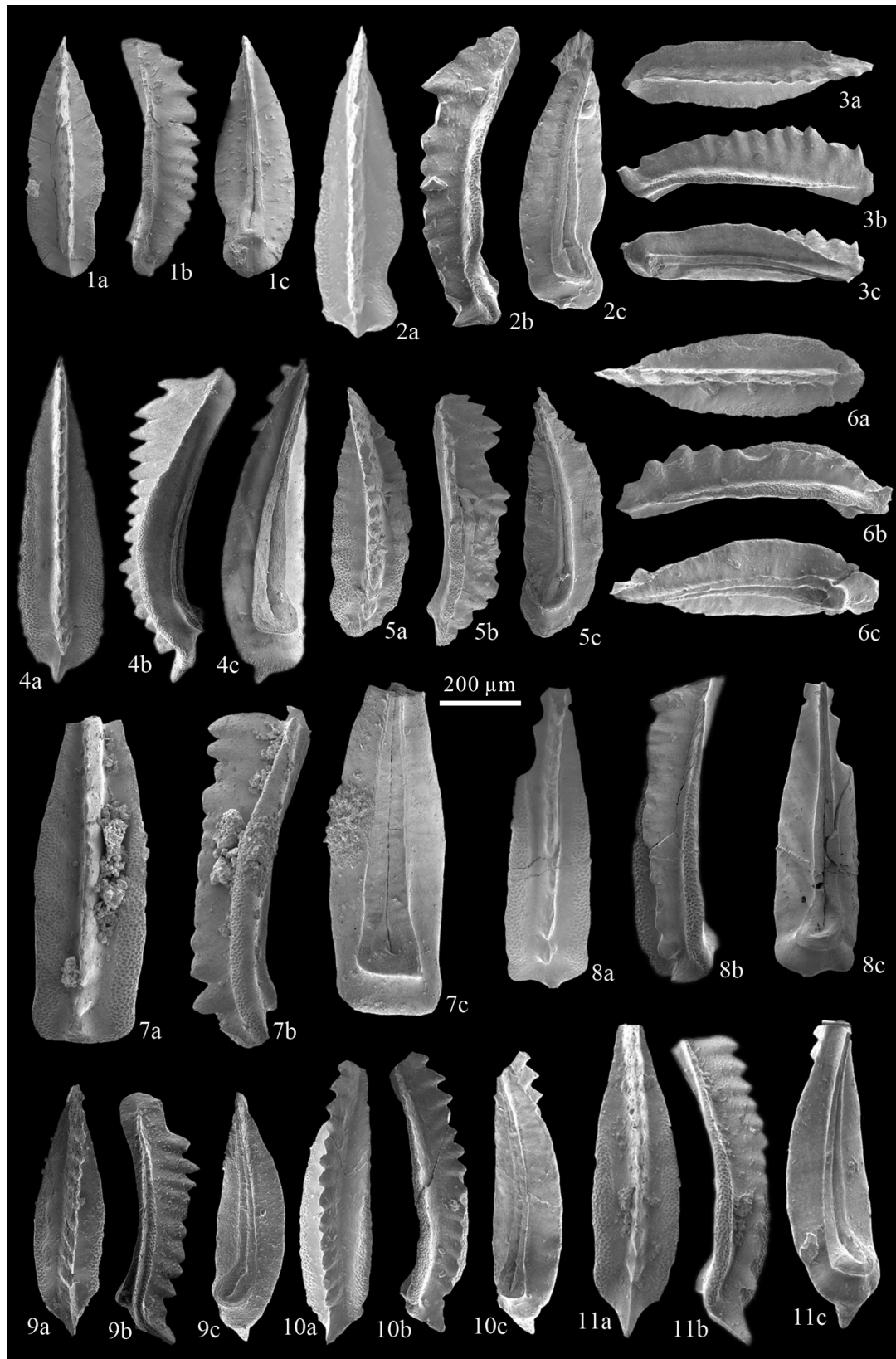
Plate 9. SEM photographs of the key conodont elements from the Shaiwa Section. 1–3. N*eogondolella curva* (Golding and Orchard, 2016), 1, 2 from Bed 19, 3 from Bed 20;1a, 2a, 3a upper view; 1b, 2b, 3b lateral view; 1c, 2c, 3c lower view; 4. *Paragondolella bulgarica* (Budurov and Stefanov, 1972), from Bed 11; 4a upper view; 4b lateral view; 4c lower view; 5. *Paragondolella excelsa* (Mosher, 1968), from Bed 35; 5a, upper view; 5b, lateral view; 5c, lower view; 6–8. *Paragondolella bifurcata* (Budurov and Stefanov, 1972), 6 from Bed 24, 7 from Bed 9, 8 from Bed 11; 6a, 7a, 8a upper view; 6b, 7b, 8b lateral view; 6c, 7c, 8c lower view; 9–11. *Neogondolella cornuta* (Budurov and Stefanov, 1972), 9, 10, 11 from Bed 33; 9a, 10a, 11a upper view; 9b, 10b, 11b lateral view; 9c, 10c, 11c lower view.